3D Finite Element Software for Cracks

Version 3.0

Benchmarks and Validation

October 2007

2465 Central Avenue, Suite 110
Boulder, CO 80301
(303) 415-1475
(303) 415-1847 (fax)
www.questreliability.com

Table of Contents

Introduction

This report compares crack results for 3D Finite Element Analysis (FEA) crack meshes generated by *FEACrack*™ to theoretical and published results. The comparison of crack results validates both the crack mesh and the analysis program computing the solution.

FEACrack is a 3D finite element crack analysis program with automatic crack mesh generation. An intuitive Windows® interface guides you step by step through the process of building the model, running the analysis, and viewing the results. The mesh generator creates complete and ready-to-run FEA input files; input files can currently be generated for *WARP3D*, *ABAQUS*, and *ANSYS*. The mesh can also be written to *FEMAP* and *PATRAN* neutral files to aid in transferring the mesh to another FEA program. Building a 3D finite element model with a crack is significantly more complicated than generating a mesh for an un-cracked component; *FEACrack* makes crack mesh generation easy.

FEACrack reads the FEA analysis results file and displays the deformed shape and color map of stress and strain results on the mesh picture, and creates x-y plots of the crack results. Additional post processing for crack values uses the J-integral results to compute elastic stress intensity K values; K is also computed from the crack opening displacements when available. Elastic-plastic J-integral results can be used to compute reference stresses and a failure assessment diagram (FAD). The crack results are displayed in several x-y plots, and the data is available in spreadsheet forms for copy-paste to other programs. Several result files can be loaded together so that crack results can be easily compared to examine the effect of changing model parameters.

Geometries used for comparison include a flat plate with buried elliptical cracks that have a theoretical solution, cylinders with internal semi-elliptical surface cracks having published solutions, through thickness cracks that have a theoretical solution, a full surface crack mesh with both crack faces, and a nozzle with a surface crack.

Finite Element Programs

WARP3D is a finite element analysis program developed at the University of Illinois and is provided with *FEACrack* as the default FEA solver program. Learn more at the *WARP3D* web page:
http://cern49.cee.uiuc.edu/cfm/warp3d.html

ABAQUS is a full-featured finite element analysis program available from *Simulia*. and must be purchased separately from *FEACrack*. Learn more at the *Simulia* products web page:
http://www.simulia.com/products/unified_fea.html

ANSYS is a full-featured finite element analysis program available from *ANSYS*, Inc. and must be purchased separately from *FEACrack*. Learn more at the *ANSYS* web page:
http://www.ansys.com

Symmetric Buried Crack

Theoretical Solution

The closed-form solution [1] for a buried elliptical crack in an infinite body subject to a uniform crack face pressure is given by:

$$K_I = G_o p \sqrt{\frac{\pi a}{Q}} \tag{2.1}$$

Where K_I is the stress intensity, G_0 is the non-dimensional geometry factor, p is the applied uniform crack face pressure, Q is the flaw shape parameter, a is the buried crack half depth, and c is the buried crack half length. The flaw shape parameter, Q, is given by:

$$Q = 1 + 1.464\left(\frac{a}{c}\right)^{1.65} \quad (a \le c) \qquad \text{Or} \qquad Q = 1 + 1.464\left(\frac{c}{a}\right)^{1.65} \quad (a > c) \tag{2.2}$$

The non-dimensional geometry factor, G_0, for the buried crack depends on the flaw aspect ratio, a/c, and the crack parametric angle, ϕ:

$$G_o = \left[\sin^2\phi + \left(\frac{a}{c}\right)^2 \cos^2\phi\right]^{1/4} \tag{2.3}$$

Figure 2-1 shows the crack dimensions and the parametric angle, ϕ, measured from the right crack tip counter clockwise around the buried crack; the full crack is length $2c$ by depth $2a$.

Since it is obviously not possible to model a crack in an infinite body with finite element analysis, a sufficiently large plate thickness was used to keep free surface effects negligible. The relative distance to the free surface, a/d_1, was set to 0.2 so that the crack depth is small compared to the plate thickness. Four crack aspect ratios a/c were used to give a range of short to long cracks, cracks with a/c of 1.0, 0.5, 0.2, and 0.1 (short to long crack lengths). In *FEACrack* a one-eighth symmetric plate with a half-thickness (d_1) of 1.0 in, a half-width of 10.0 in, and a half-depth of 10.0 in was used for the buried crack meshes. The buried crack depth $2a$ is 0.4 in (a is 0.2), and the buried crack lengths $2c$ are: 0.4, 0.8, 2.0, and 4.0, corresponding to the four a/c crack aspect ratios. The uniform crack face pressure p is 1000 psi. Since the non-dimensional stress intensity values will be compared, other meshes that use the same relative crack dimensions will give the same non-dimensional results. The characteristic stress is the uniform crack face pressure when computing G_0.

Figures 2-2, 2-3, and 2-4 show a few crack mesh pictures for the symmetric buried crack mesh generated by *FEACrack*. Appropriate boundary conditions for the symmetry planes are applied to the left, top, and front surfaces of the mesh.

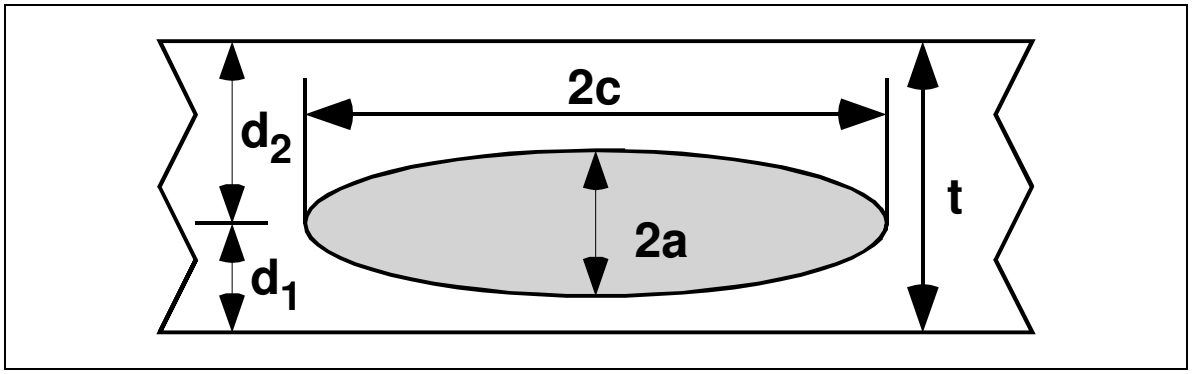

Figure 2-1 (a). Buried crack geometry dimensions.

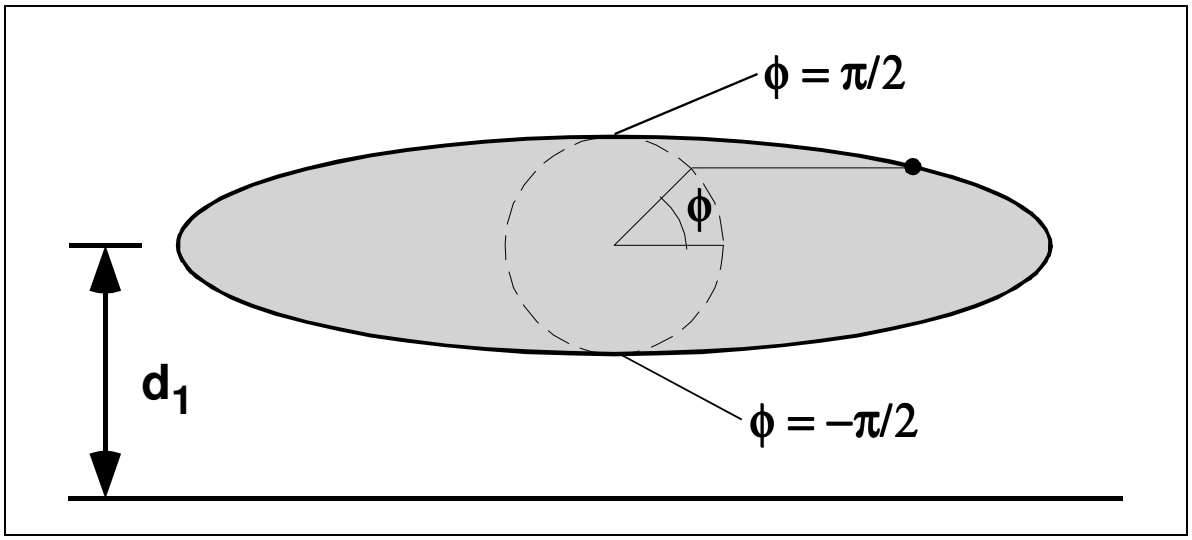

Figure 2-1 (b). Buried crack geometry parametric crack angle ϕ.

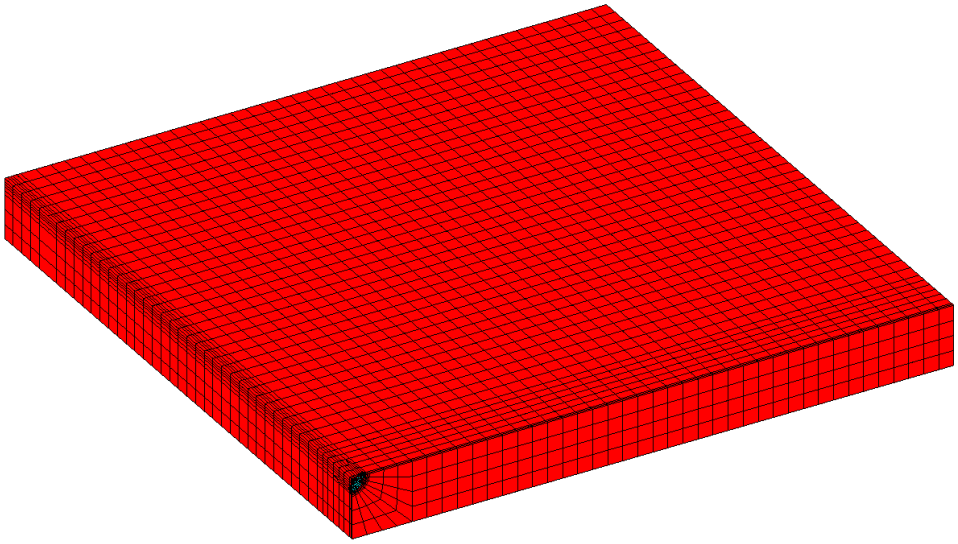

Figure 2-2. Symmetric buried crack modeled by a one-eighth symmetric plate mesh.

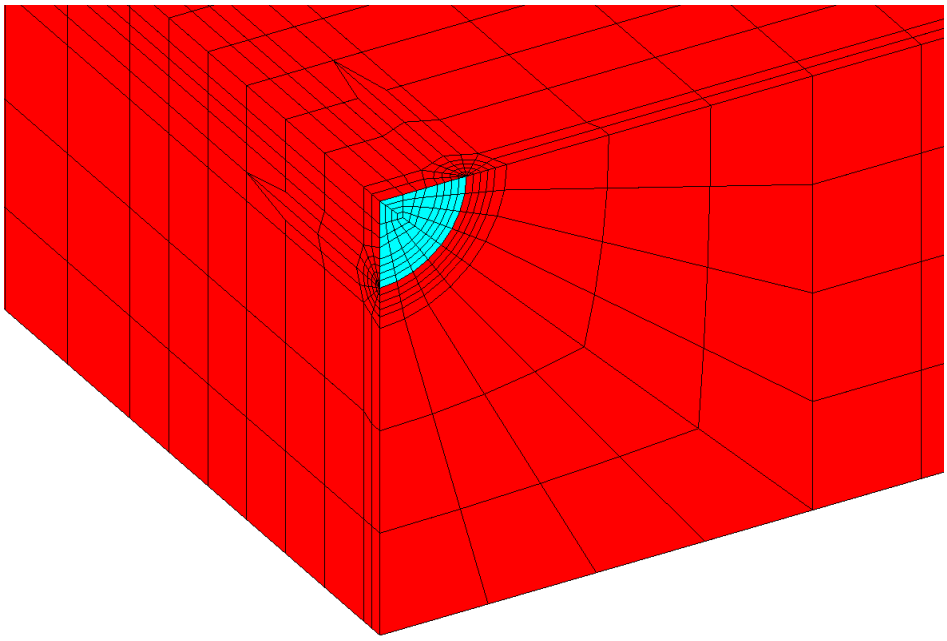

Figure 2-3. Symmetric buried crack close up; a/d_1 = 0.2, a/c = 1.0.

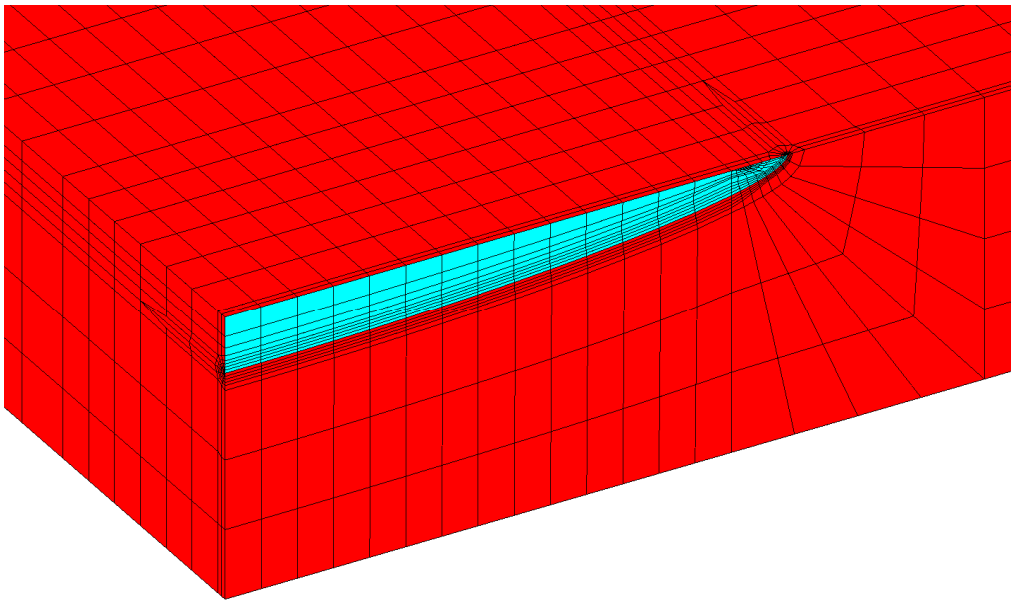

Figure 2-4. Symmetric buried crack close up; a/d_1 = 0.2, a/c = 0.1.

Post Processing Equations

Several more equations are listed here that are used when examining crack results and to compute related crack values. For mode I crack opening the J-integral results can be converted to an equivalent elastic stress intensity K_I.

$$K_I = \sqrt{\frac{JE}{1-\nu^2}} \tag{2.4}$$

Where J is the computed J-integral results, E is the Young's modulus of elasticity, and v is the Poisson ratio. Using equation (2.4) to compute K from J then permits the non-dimensional stress intensity, G_0, to be computed using equation (2.1) for comparison to other results.

Using the crack opening displacements the mode I crack opening stress intensity K_I can be computed along the crack using two equations depending on the crack shape being analyzed. For a surface crack use a plane stress assumption at the free surface crack tip ($\phi = 0$):

$$K_I = 0.25E\left(\frac{U_{\text{crack}}}{2}\right)\left(\frac{2\pi}{R}\right)^{1/2} \tag{2.5}$$

Where U_{crack} is the total crack opening displacement and R is the radial distance on the crack face from the crack node to other crack face nodes. Note that the crack mesh has been generated so that mesh lines are normal to the crack curve. Along the surface crack front ($\phi > 0$) or for a buried crack use a plane strain assumption:

$$K_I = \frac{0.25E\left(\frac{U_{\text{crack}}}{2}\right)\left(\frac{2\pi}{R}\right)^{1/2}}{1-v^2} \tag{2.6}$$

The J-integral result values can be evaluated by checking the contour integral path dependence index; this value is reported on the crack results data window in *FEACrack*. The contour integral path dependence index, d, is computed using:

$$d = \frac{J_{\max} - J_{\min}}{2J_{\text{avg}}} \tag{2.7}$$

Where $J_{\max}$ is the largest J-integral contour value, $J_{\min}$ is the smallest contour value, and J_{avg} is the average of the contour values. Usually the first contour is discarded when computing the path dependence index and J_{avg} as it is usually not very accurate. Using 4 or 5 contours is recommended for *FEACrack* meshes. Path dependence index values below 0.05 are considered to show low path dependence in the J-integral results.

Buried Crack WARP3D Results

Four *WARP3D* format crack mesh input files for the crack aspect ratios *a/c* of 1.0, 0.5, 0.2, 0.1 were generated by *FEACrack* to analyze the symmetric buried crack. The computed J-integral results were used to compute K_I, and the crack opening displacement was used to compute K_I for comparison. The K-from-J values were then used to compute the non-dimensional stress intensity for comparison to the theoretical values shown in Figure 2-5. The *WARP3D* non-dimensional stress intensity results generally compare within 2% of the theoretical solution.

The comparison of K values computed from the J-integral results and from the crack opening displacement is shown in Figure 2-6. Using K from displacement provides an independent value to verify K from the J-integral results. The K from displacement was computed for each crack node using equation (2.6) for the buried crack. K from displacement values are computed for the crack face nodes along the radial mesh line from the crack node. The trend of K versus the distance from the crack node is used for a least-square fit to obtain the K value at the crack node at a radial distance of zero. The plot shows very good agreement for *a/c* of 1.0 and 0.5. The curves do not agree quite as closely near the right end of the buried crack ($\phi = 0$)

for the longer cracks, *a/c* = 0.2 and 0.1 but do verify the trend along the crack front. The results at the right end of the crack (most crack curvature) could be improved by increasing the mesh refinement along the crack front (3x or 9x options available in *FEACrack*).

The close agreement between the *WARP3D* FEA and theoretical results verifies that a good crack mesh is being generated by *FEACrack* and good results are being computed and obtained from the *WARP3D* result file.

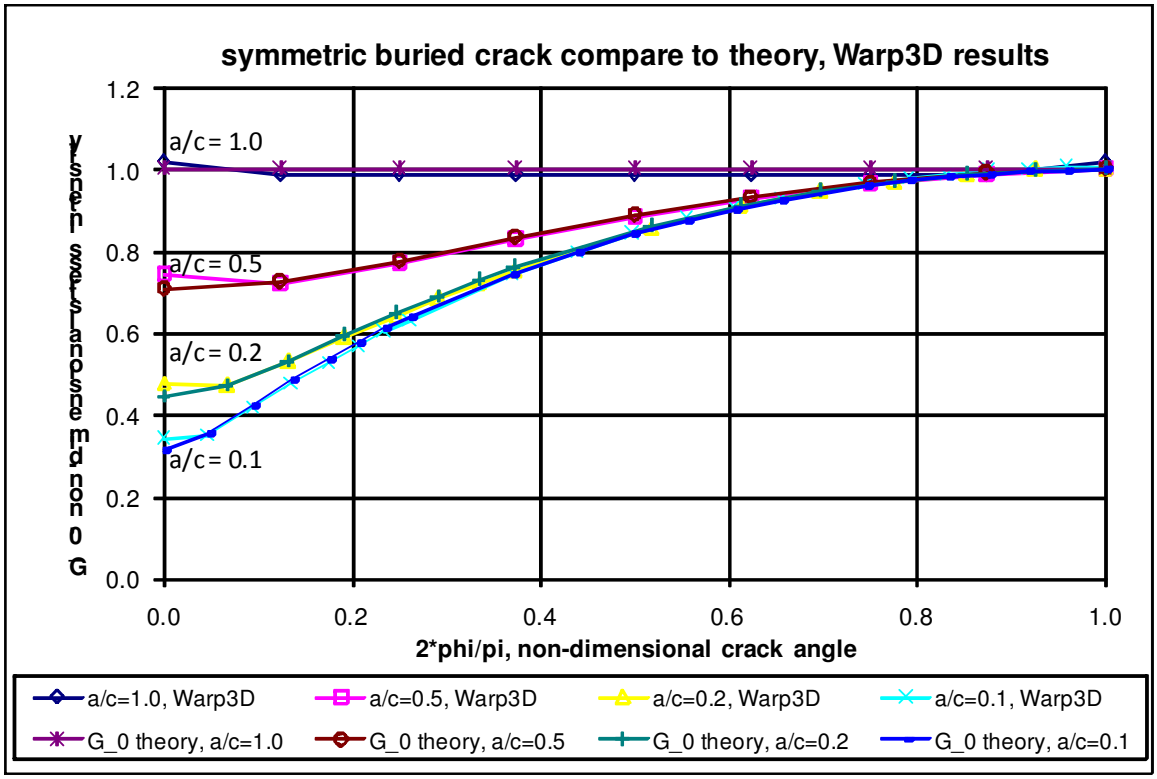

Figure 2-5. Compare *WARP3D* results to theory for the symmetric buried crack with uniform crack face pressure and four crack sizes

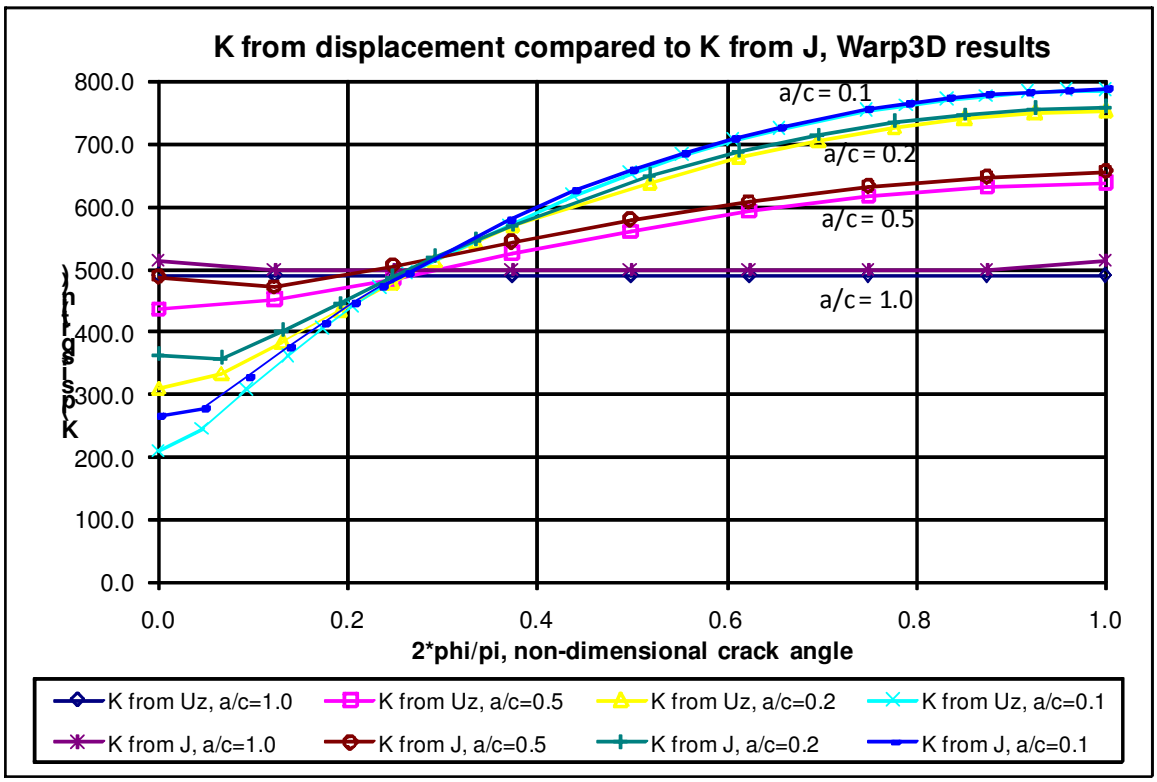

Figure 2-6. Compare K from J-integral and K from crack opening displacement *WARP3D* results.

Buried Crack ABAQUS Results

Like the *WARP3D* result comparisons in the previous section, four *ABAQUS* crack mesh input files were generated by *FEACrack* for the symmetric buried crack aspect ratios *a/c* of 1.0, 0.5, 0.2, and 0.1. The comparison of the non-dimensional stress intensity results is shown in Figure 2-7. The FEA results from *ABAQUS* agree closely with the theoretical buried crack solution. The comparison of *K* from J-integral and crack opening displacement results is shown in Figure 2-8. The *K* values compare very well for the shorter cracks, *a/c* of 1.0 and 0.5, but not quite as good for the longer cracks, *a/c* of 0.2 and 0.1.

Using the 3X (three times) crack front mesh refinement option in *FEACrack* the four buried crack meshes were regenerated and analyzed. The comparison of non-dimensional stress intensity results is shown in Figure 2-9; the comparison of K from J and crack opening displacement is shown in Figure 2-10. The results are improved near the right end of the crack ($\phi = 0$) where the crack front curvature is greatest, and the results are somewhat improved for the longer cracks (smaller *a/c* crack aspect ratios). The additional mesh refinement helps to better follow the curved crack front elliptical curve.

The close agreement between the *ABAQUS* FEA and theoretical results verifies that a good crack mesh is being generated by *FEACrack* and good results are being computed and obtained from the *ABAQUS* result file.

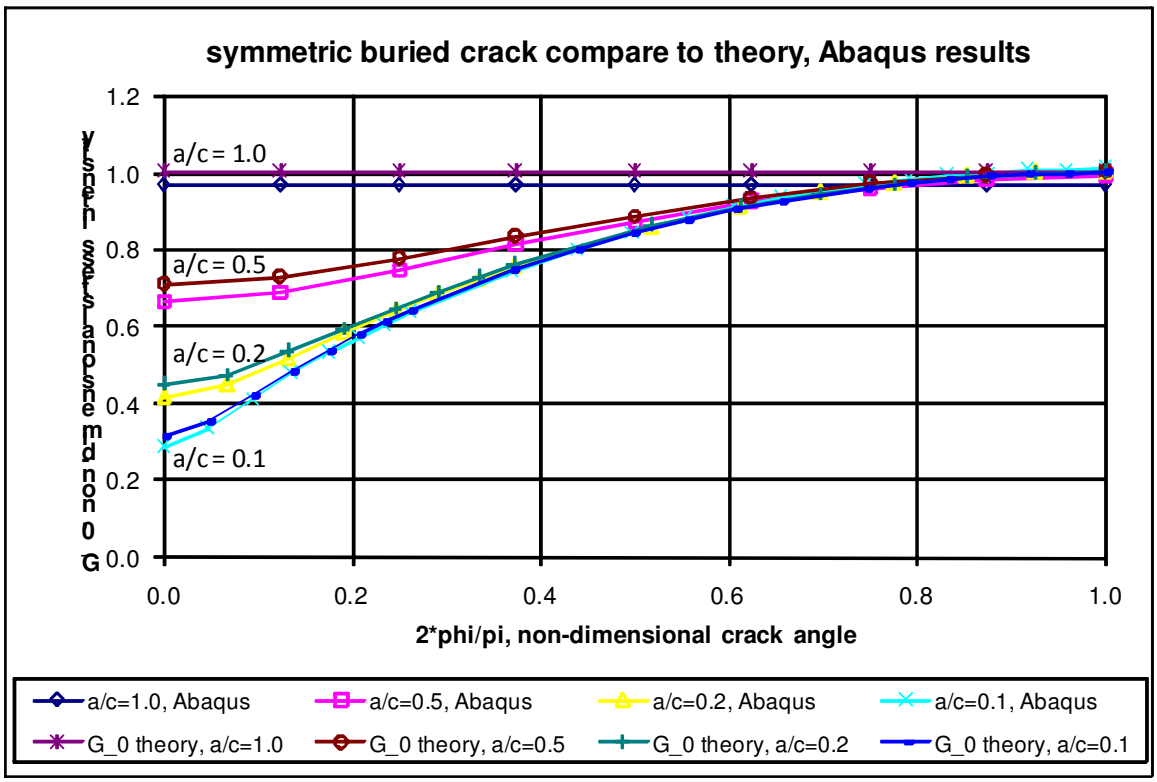

Figure 2-7. Compare *ABAQUS* results to theory for the symmetric buried crack.

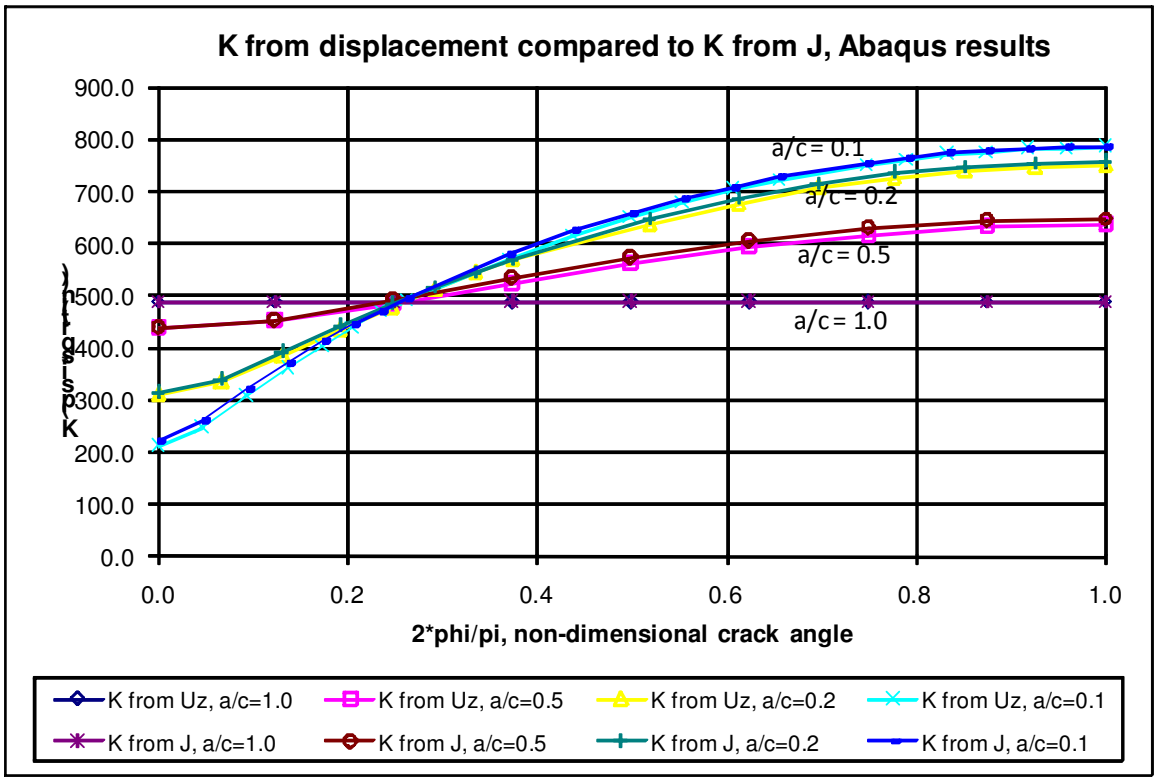

Figure 2-8. Compare K from J-integral and crack opening displacement *ABAQUS* results.

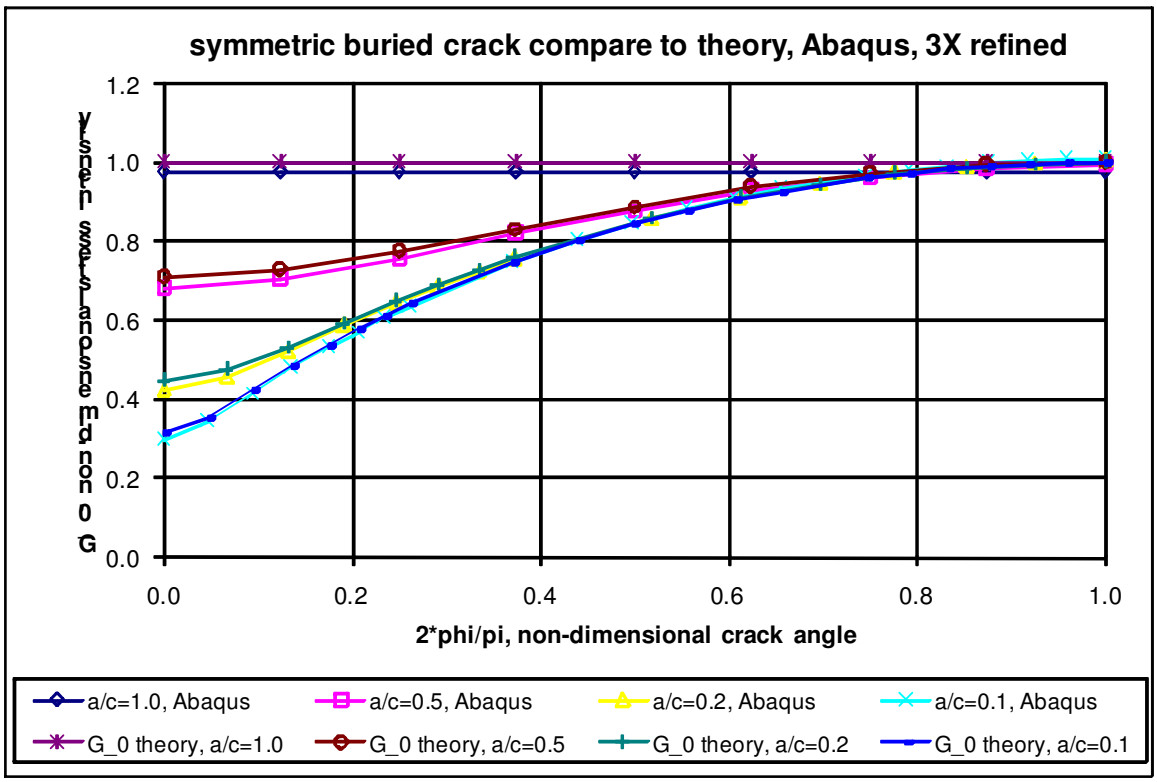

Figure 2-9. Compare *ABAQUS* results to theory, symmetric buried crack, 3X crack front refinement

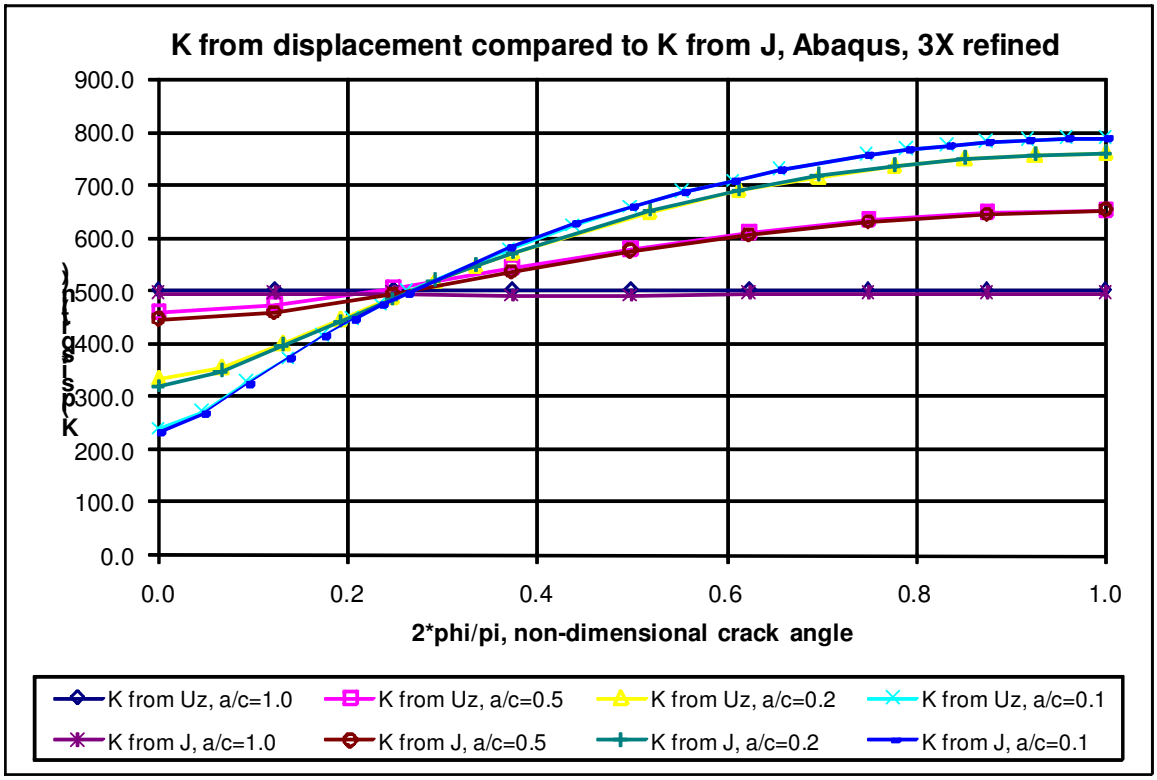

Figure 2-10. Compare K from J-integral and crack opening displacement *ABAQUS* results, the crack front has 3X mesh refinement

Buried Crack ANSYS Results

As in the previous sections, four *ANSYS* crack mesh input files were generated by *FEACrack* for the symmetric buried crack aspect ratios *a/c* of 1.0, 0.5, 0.2, and 0.1. The comparison of the non-dimensional stress intensity results is shown in Figure 2-11. The crack result values computed by the Quest Reliability LLC ("QR" for short) J-integral post-processing module using *ANSYS* results agree closely with the theoretical buried crack solution. Since *ANSYS* does not support the J-integral, the *FEACrack* post-processor uses the Gauss integration point results from the *ANSYS* .rst file to compute the crack front J-integral. The comparison of K-from-J and crack opening displacement results is shown in Figure 2-12. The *K* values compare very well for the shorter cracks, *a/c* of 1.0 and 0.5, but not quite as good for the longer cracks, *a/c* of 0.2 and 0.1.

The close agreement between the *ANSYS* FEA and theoretical results verifies that a good crack mesh is being generated by *FEACrack* and good results are being computed and obtained from the *ANSYS* result file. The J-integral being computed by the Quest Reliability J-integral module using *ANSYS* results is correct.

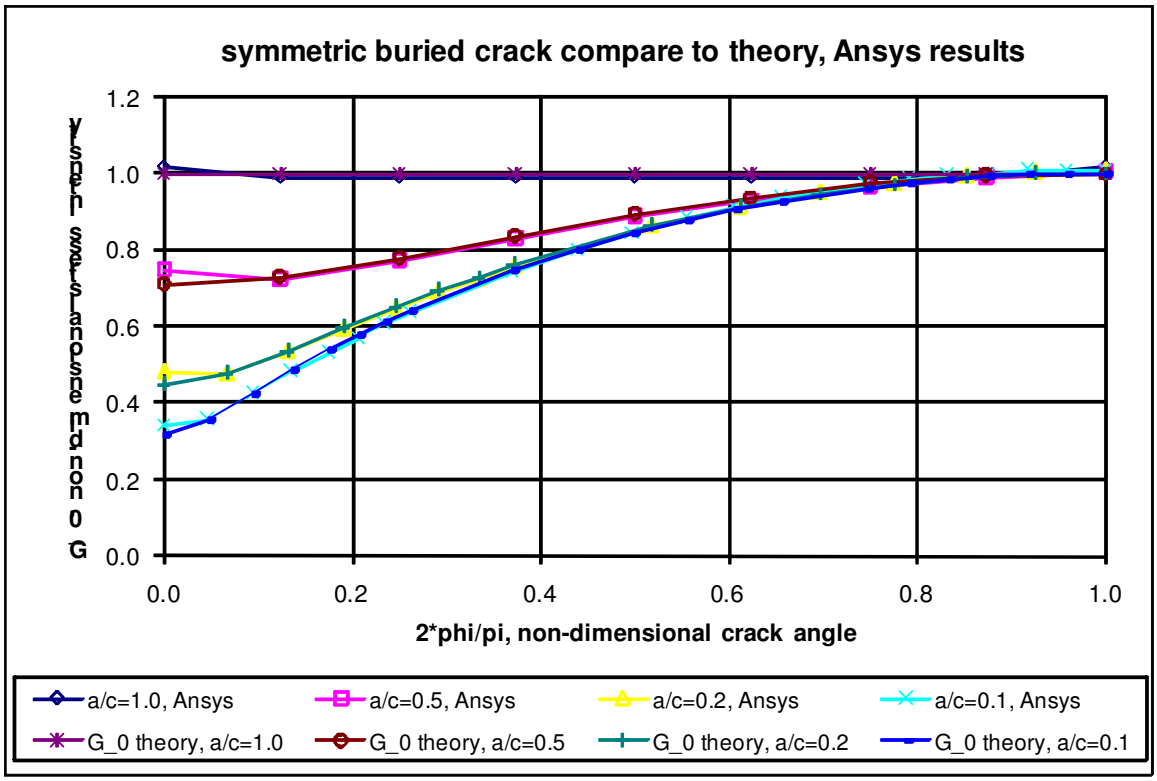

Figure 2-11. Compare *ANSYS* results to theory for the symmetric buried crack.

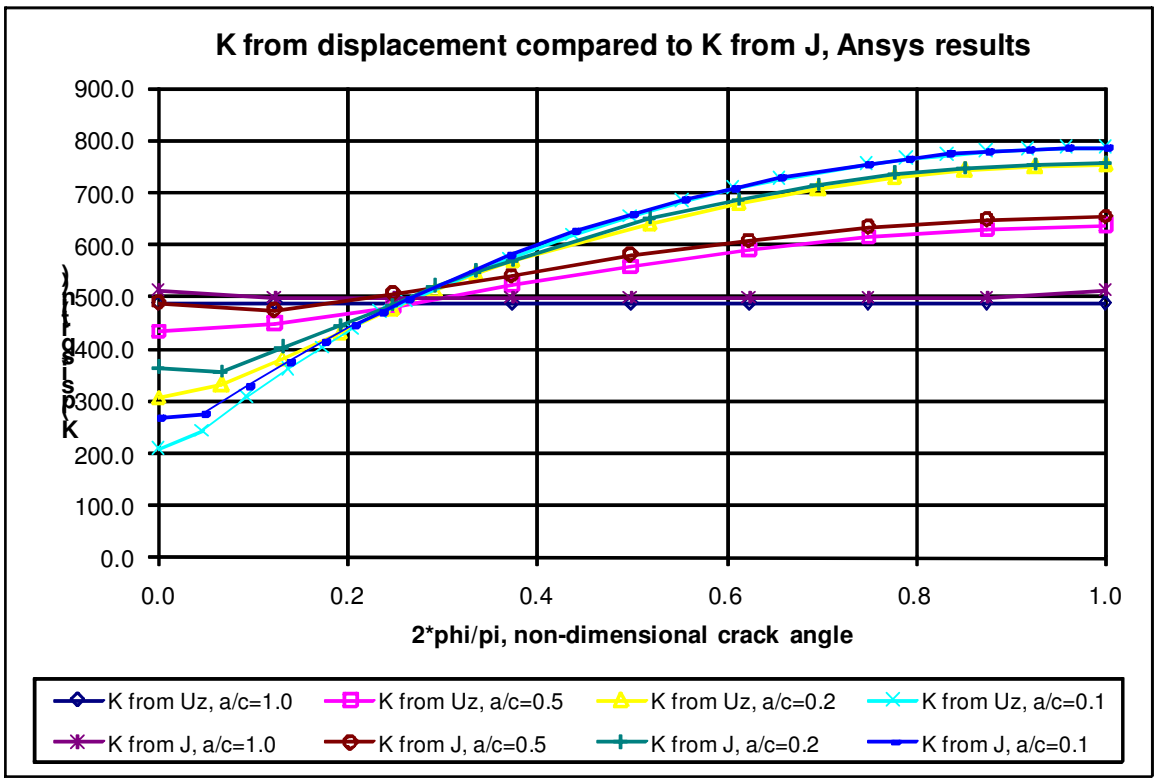

Figure 2-12. Compare K from J-integral and crack opening displacement *ANSYS* results.

QR J-integral Module and Buried Crack Results

The J-integral post-processing calculation module developed at Quest Reliability (QR) can use displacement, stress, and strain results from a FEA program to compute the J-integral along a crack. Using the results for the buried crack presented in the previous sections, the J-integral computed by the QR J-integral module using *WARP3D* and *ABAQUS* results can be compared to the J-integral values computed by those programs. Since *ANSYS* does not have J-integral results, the crack results computed using *ANSYS* FEA result values and the QR J-integral module have already been presented in the previous *ANSYS* results section.

The J-integral results for the buried crack from *WARP3D* and from the QR J-integral module using the displacement, stress, and strain results from *WARP3D* are shown in Figure 2-13. The J-integral results for the same buried crack meshes from *ABAQUS* and the QR J-integral module using *ABAQUS* results are shown in Figure 2-14. In both plots the J-integral computed by the QR J-integral module agrees very closely with the J-integral results obtained from the *WARP3D* or *ABAQUS* result files. This verifies that the J-integral calculations are correct in the QR module and that the QR module can be used with other FEA programs that do not have J-integral results.

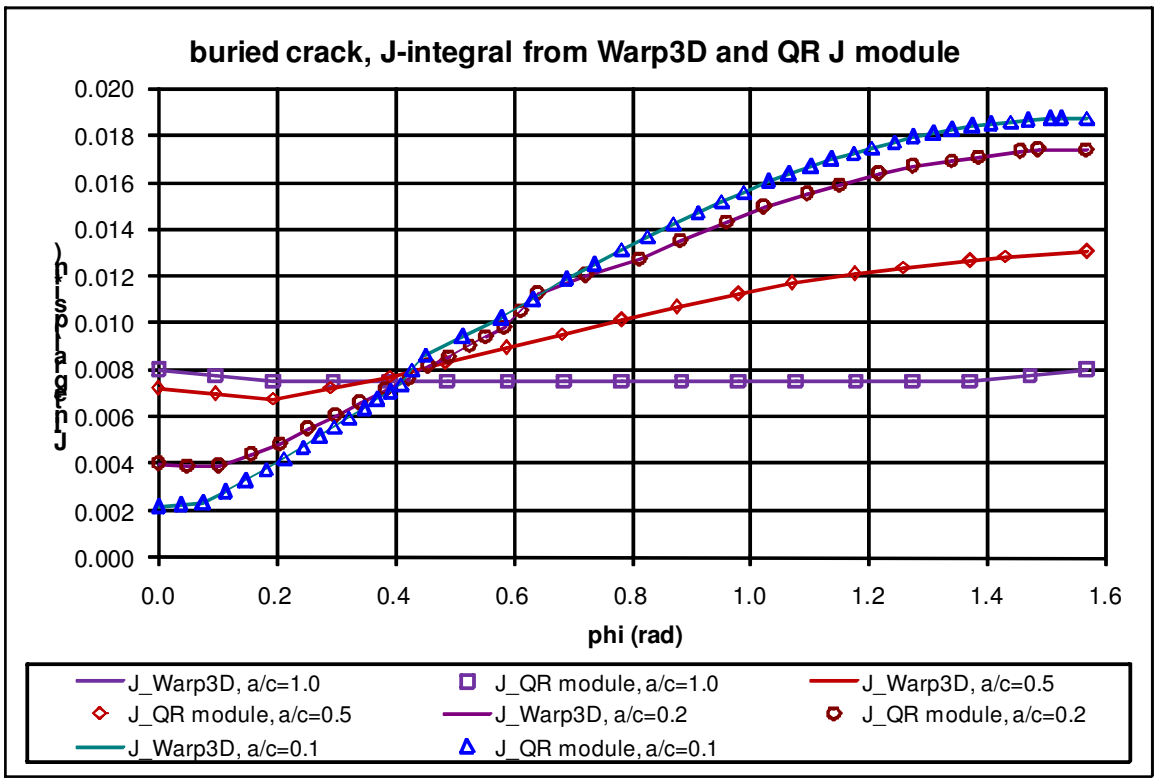

Figure 2-13. Compare buried crack J-integral results from *WARP3D* and the QR J-integral module.

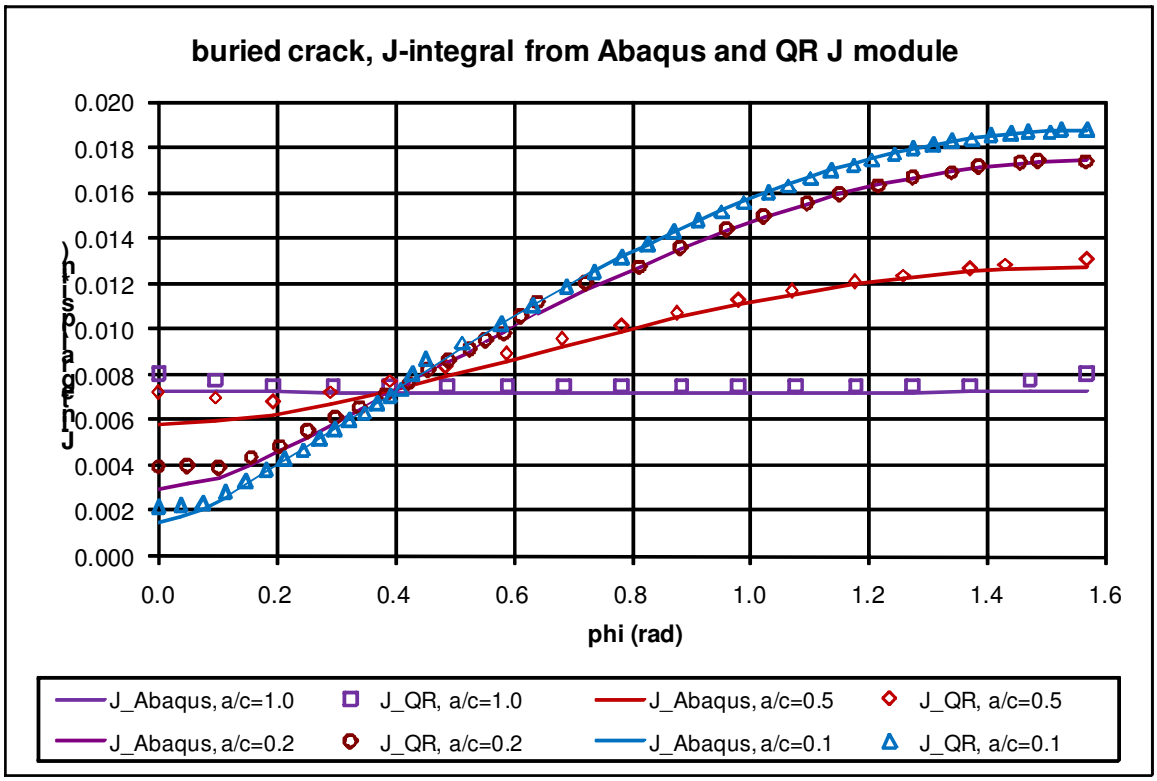

Figure 2-14. Compare buried crack J-integral results from *ABAQUS* and the QR J module.

Cylinder Surface Cracks

Bergman [2] has published stress intensity results for circumferential surface cracks in cylinders with R_i/t ratios of 5 and 10; where R_i is the cylinder inside radius and t is the cylinder wall thickness, see Figure 3-1 for cylinder and crack dimensions. He used his own mesh generator along with the *ABAQUS* commercial finite element program. He fit the non-dimensional stress intensity to a 6th-order polynomial. The polynomial curve fit coefficients are also available from *FEACrack*. The 6th order curve fit polynomial is given by the equation:

$$G_n(\phi) = A_o + A_1\left(\frac{2\phi}{\pi}\right) + A_2\left(\frac{2\phi}{\pi}\right)^2 + A_3\left(\frac{2\phi}{\pi}\right)^3 + A_4\left(\frac{2\phi}{\pi}\right)^4 + A_5\left(\frac{2\phi}{\pi}\right)^5 + A_6\left(\frac{2\phi}{\pi}\right)^6 \qquad (3.1)$$

Where the seven curve fit coefficients are A_0 through A_6, and ϕ is the surface crack front angle, see Figure 3-1. This curve fit polynomial equation is valid for the range $0 \le \phi \le \pi/2$ (from the crack tip to the deepest point of the crack).

In the Bergman paper, the relative crack sizes have *a/t* ratios of 0.2 and 0.8 (shallow and deep crack cases), and *a/c* ratios of 1, 0.25, and 0.0625 for increasing crack length (or *c/a* of 1, 4, and 16). The applied loading cases on the crack face are a uniform pressure and a linear pressure profile. The crack face pressure is given by the equation:

$$p(x) = p_n\left(\frac{x}{a}\right)^n \qquad (3.2)$$

Where a is the crack depth, x is the distance from the top of the crack toward the crack depth, and the exponent n gives the crack face pressure profile; n is zero for uniform crack face pressure, and n is 1 for linear crack face pressure, see Figure 3-2.

Figures 3-3 through 3-9 show crack mesh pictures for the quarter symmetric cylinder with an internal circumferential surface crack generated by *FEACrack*. Appropriate boundary conditions for the symmetry planes are applied to the left end of the cylinder and on the top and bottom of the mesh in the x-y plane.

The non-dimensional stress intensity, G_0, results from the *FEACrack* cylinder surface crack meshes are compared in the following sections for each FEA program.

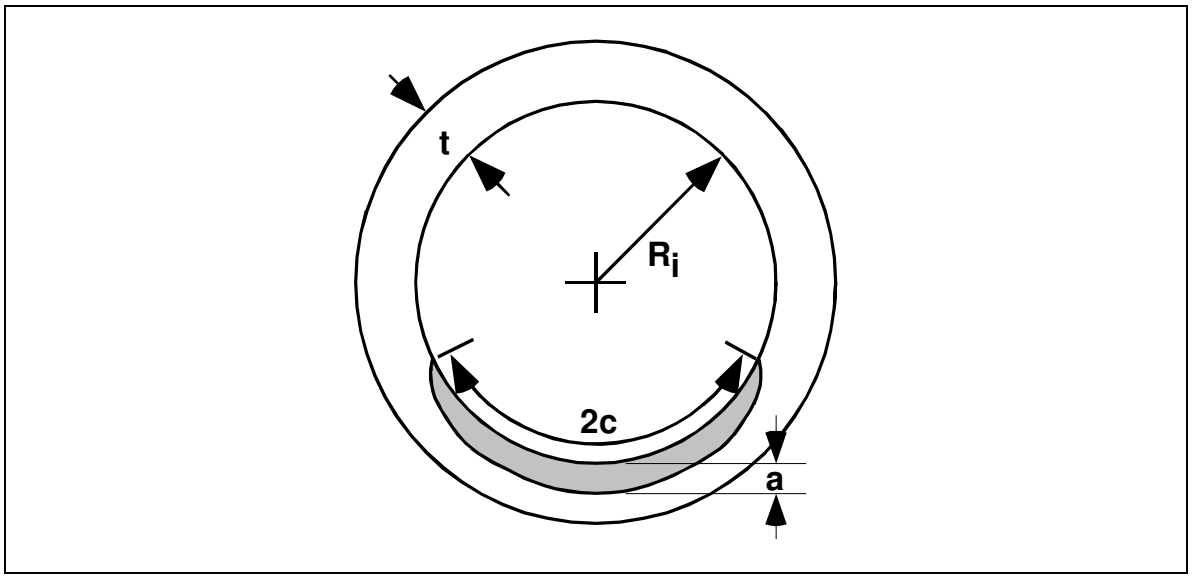

Figure 3-1 (a). Internal circumferential crack in a cylinder, crack and cylinder dimensions.

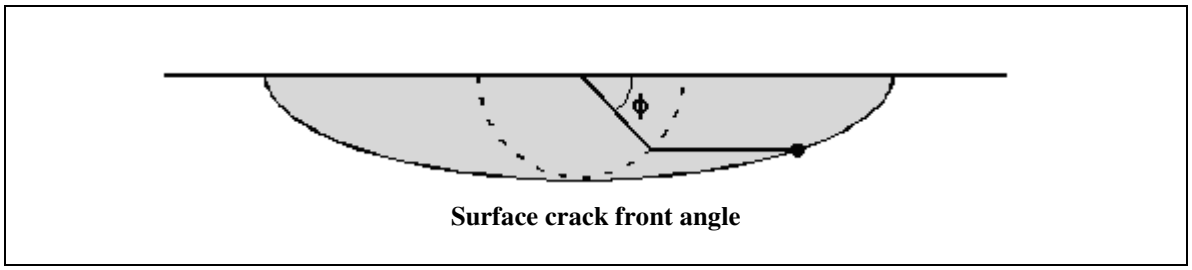

Figure 3-1 (b). Surface cracks in cylinders, crack front angle ϕ.

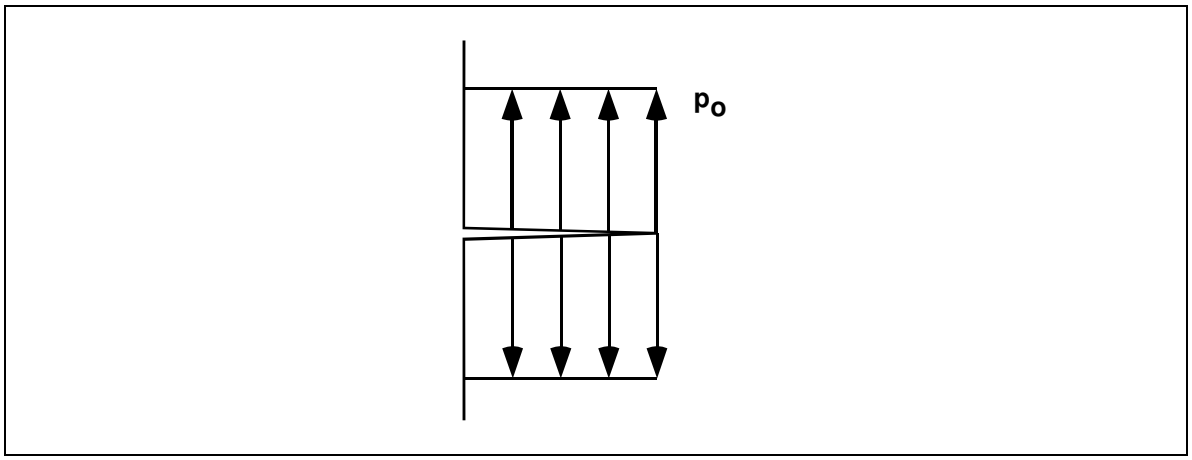

Figure 3-2 (a). Uniform crack face pressure, $p(x) = p_o$

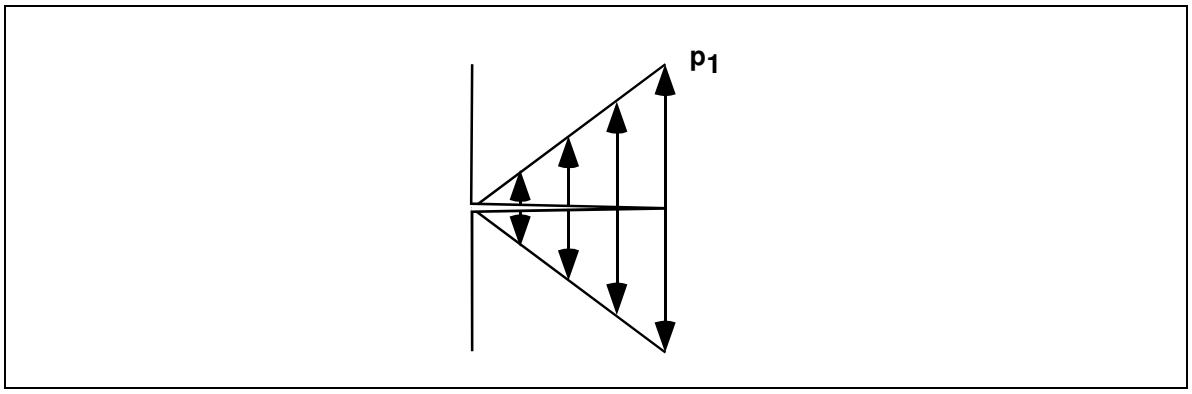

Figure 3-2 (b). Linear crack face pressure, $p(x) = p_1\left(\frac{x}{a}\right)$

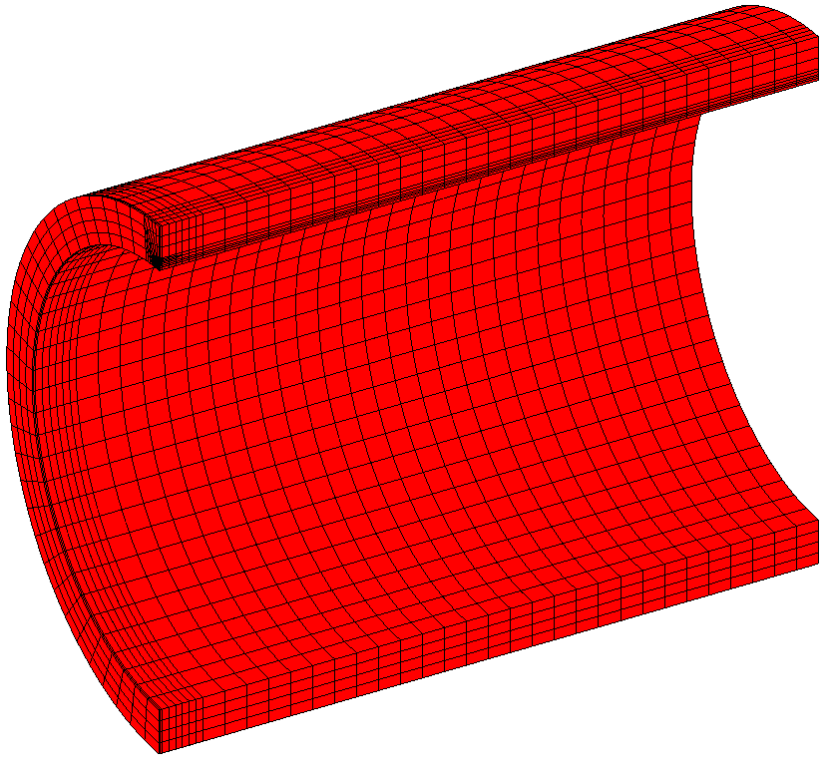

Figure 3-3. Cylinder with an internal circumferential surface crack, Ri/t = 5

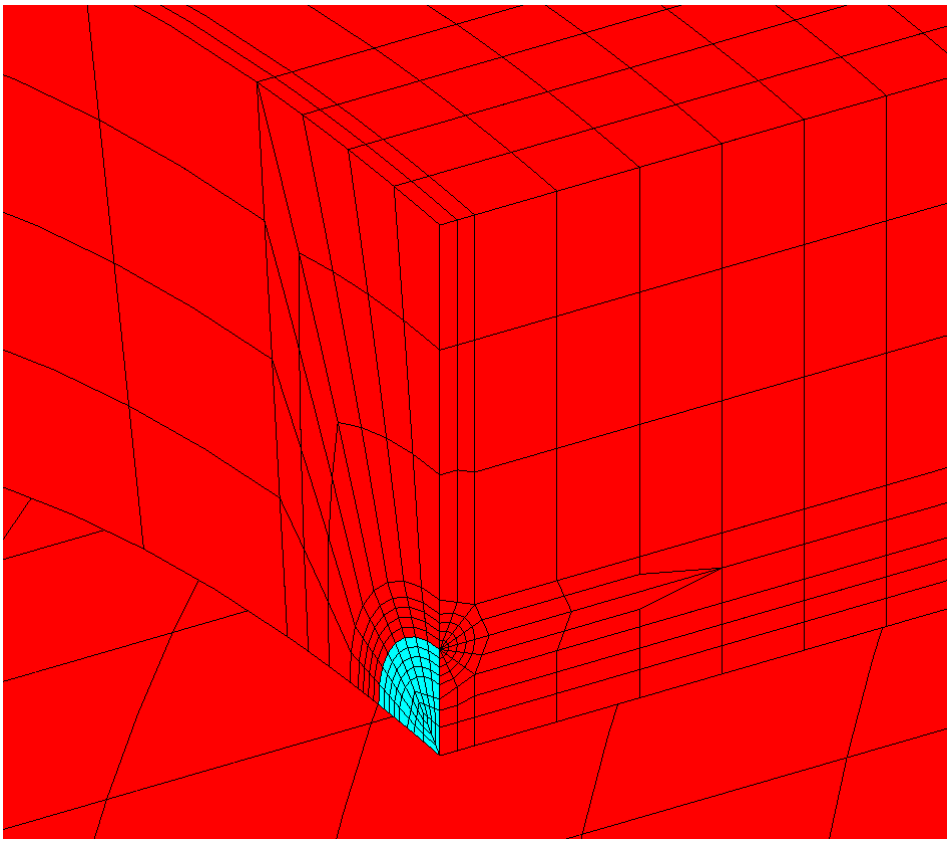

Figure 3-4. Cylinder with an internal circumferential surface crack, a/t = 0.2, a/c = 1

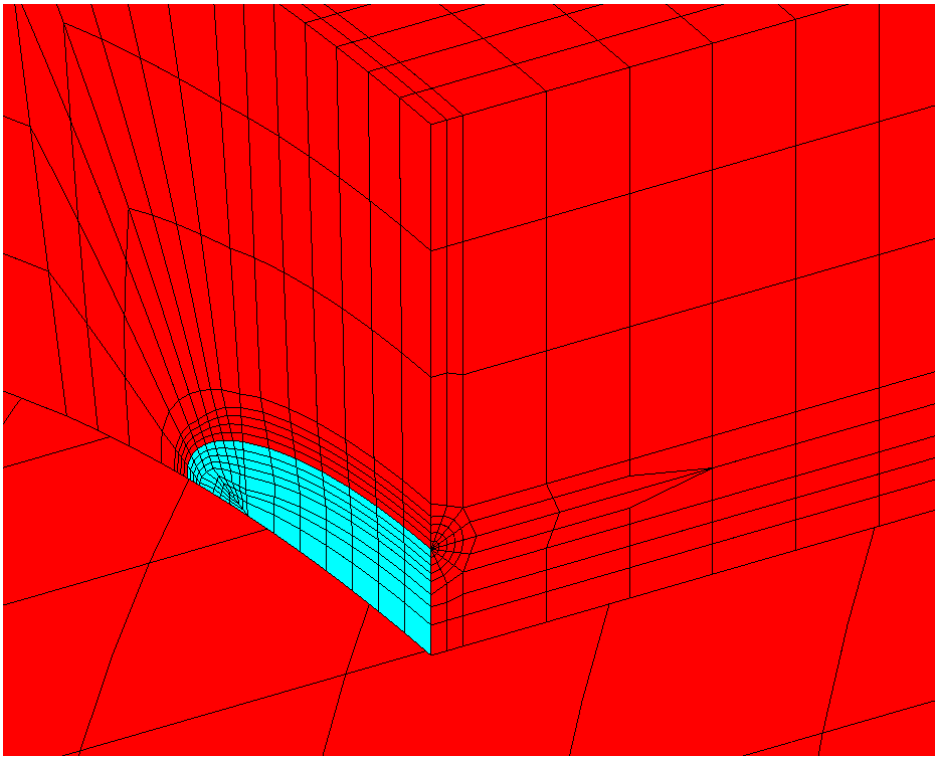

Figure 3-5. Cylinder with an internal circumferential surface crack, a/t = 0.2, a/c = 0.25

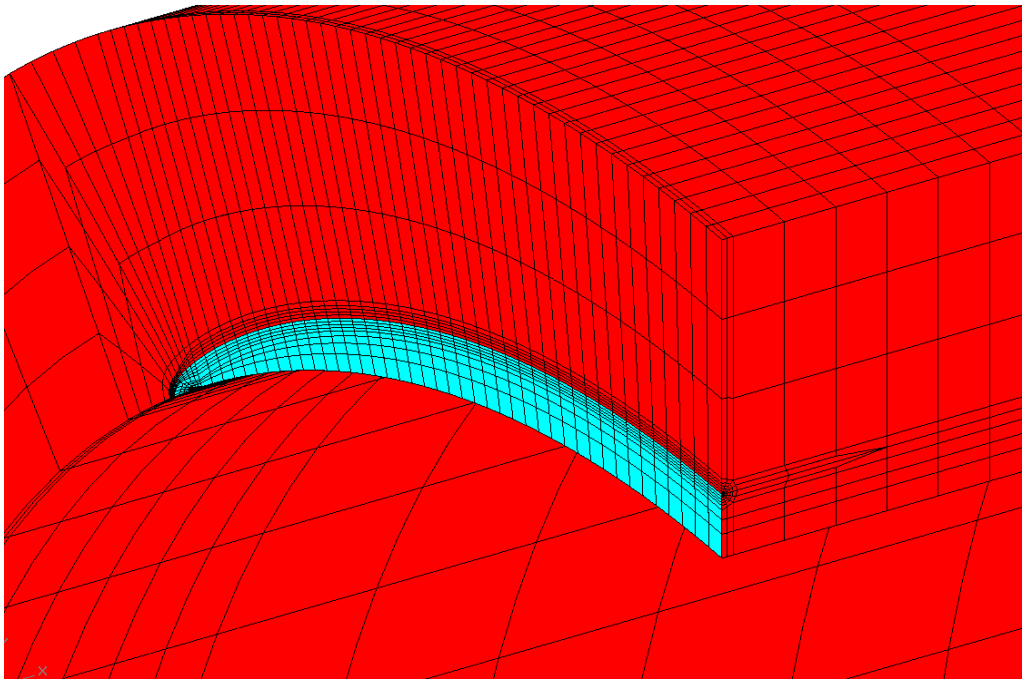

Figure 3-6. Cylinder with an internal circumferential surface crack, a/t = 0.2, a/c = 0.0625

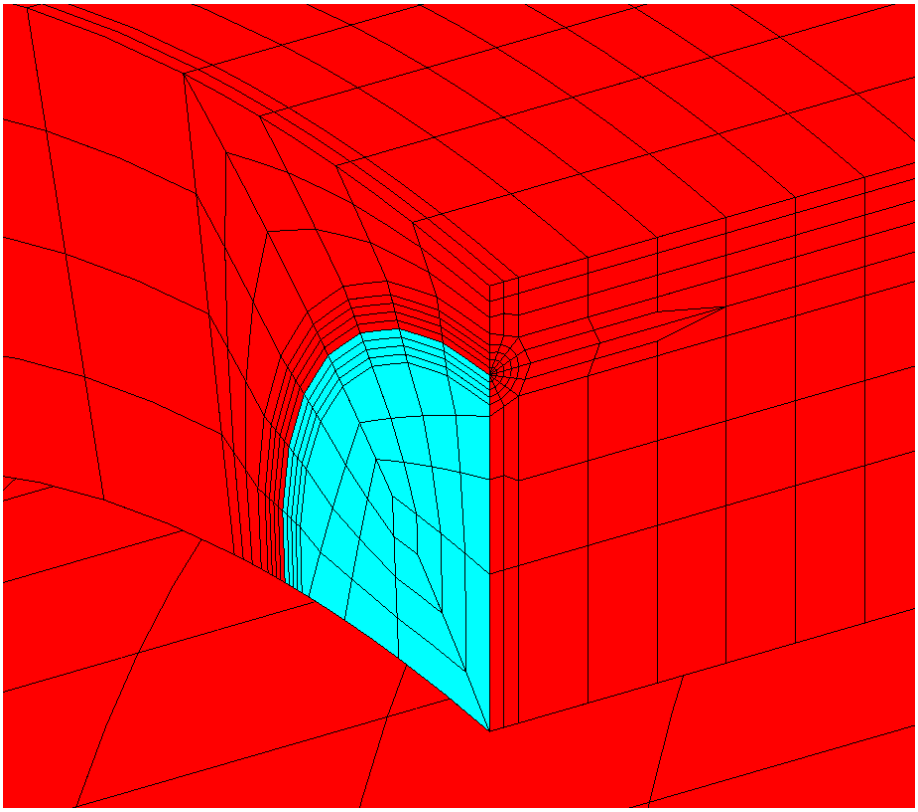

Figure 3-7. Cylinder with an internal circumferential surface crack, a/t = 0.8, a/c = 1.0

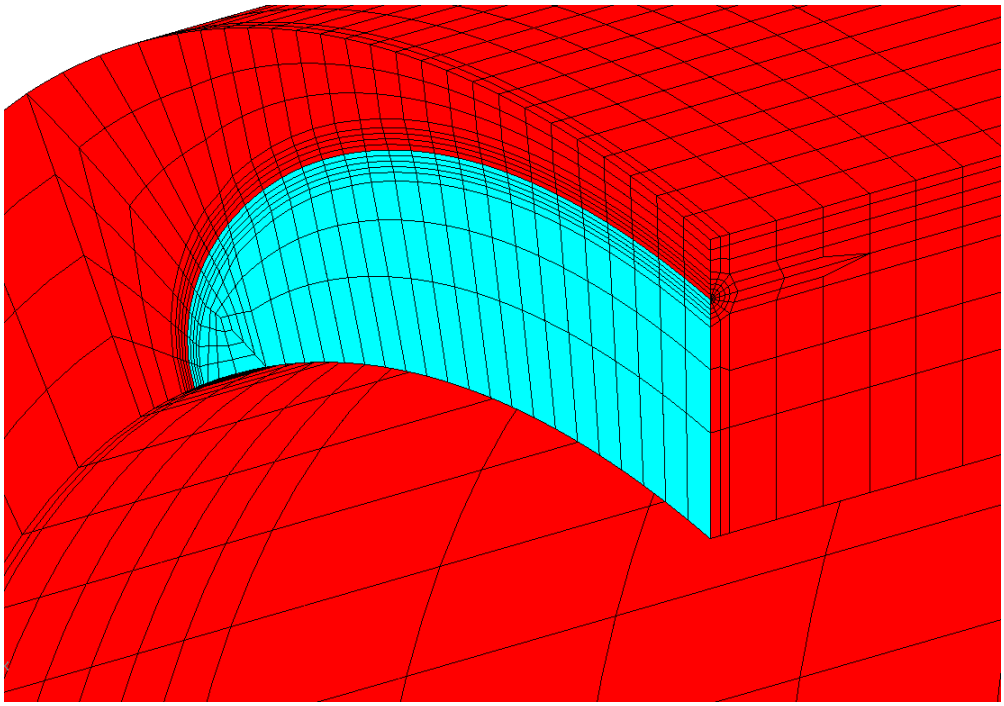

Figure 3-8. Cylinder with an internal circumferential surface crack, a/t = 0.8, a/c = 0.25

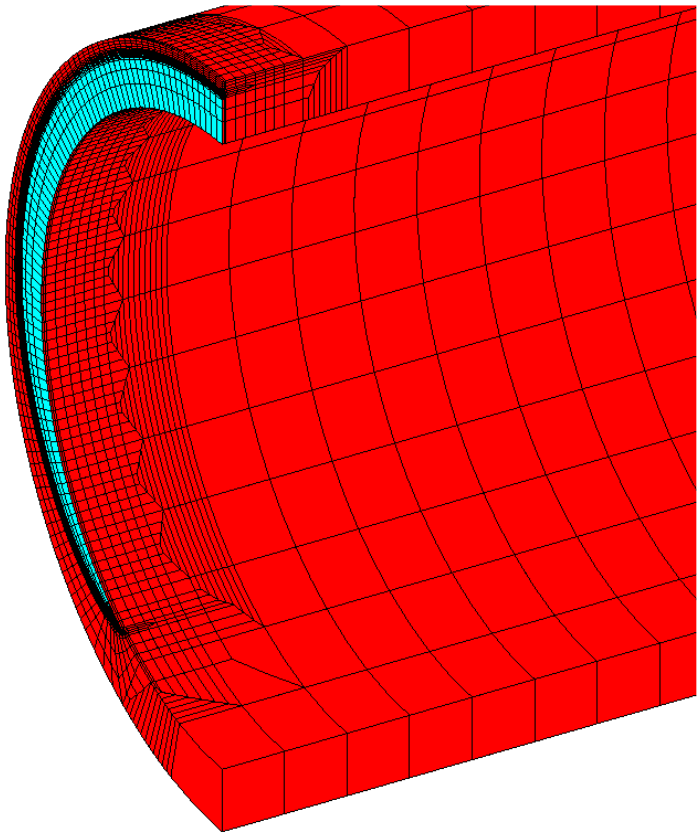

Figure 3-9. Cylinder with an internal circumferential surface crack, a/t = 0.8, a/c = 0.0625

Cylinder Surface Cracks WARP3D Results

Groups of three *WARP3D* crack mesh input files were generated by *FEACrack* for the cylinder internal circumferential surface crack aspect ratios *a/c* of 1.0, 0.25, and 0.0625. The crack depth ratio for each set of crack meshes *a/t* is 0.2 and 0.8. Uniform and linear crack face pressure loading is used for each set of crack meshes. The cylinder values used for these analyses are inside radius R_i of 5.0 in, thickness *t* of 1.0 in, cylinder length *L* of 15.0 in, and maximum crack face pressure magnitude *p* of 1000 psi. The material values used are Young's modulus of elasticity, *E*, of 30×10^6 psi, and Poisson's ratio, *v*, of 0.3. The comparison of the non-dimensional stress intensity results to the Bergman results is shown in Figures 3-10 through 3-13.

The FEA results from *WARP3D* using the *FEACrack* crack meshes agree closely with the Bergman solutions; also refer to the additional discussion in the next *ABAQUS* results section. The results show that a good crack mesh is being generated by *FEACrack* and that *WARP3D* is computing the correct solution. The local drop in the a/c=0.25 curve from Warp3D appears due to the change in element size; a small element on one side of the crack front node to a larger element on the other side of the crack front node at the mesh block boundary.

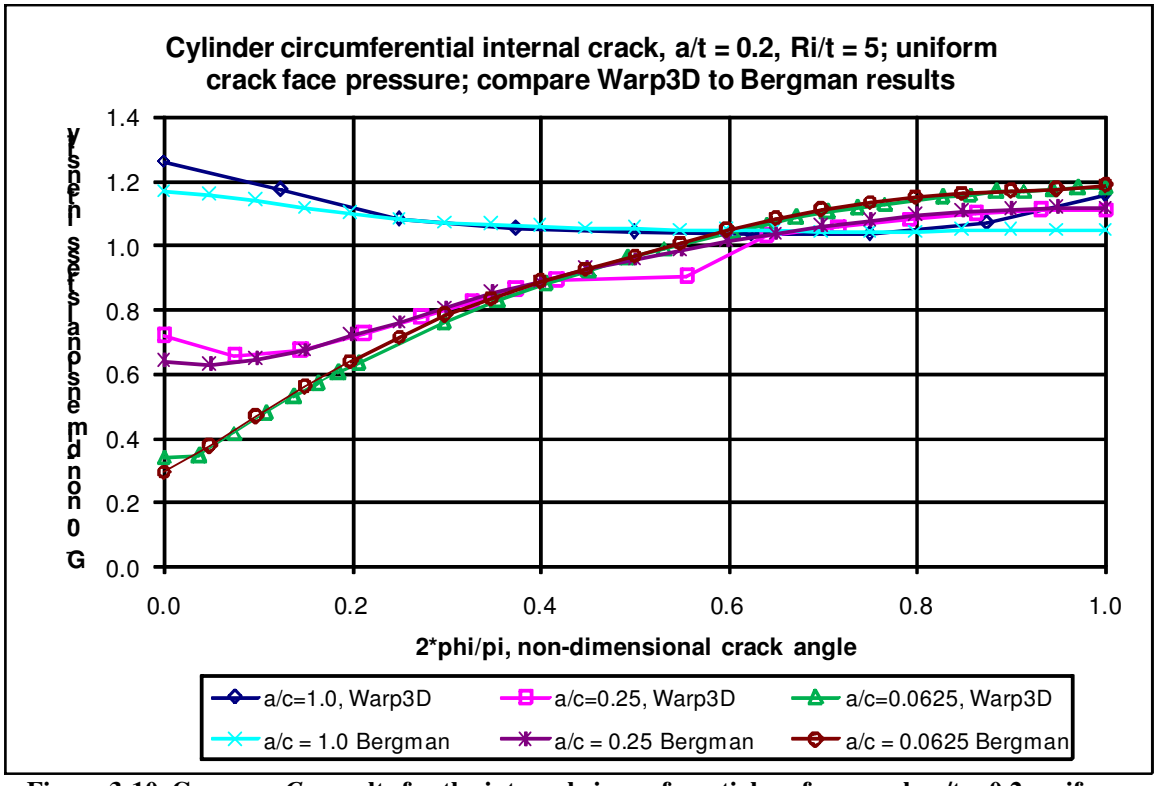

Figure 3-10. Compare G_0 results for the internal circumferential surface crack, a/t = 0.2, uniform crack face pressure

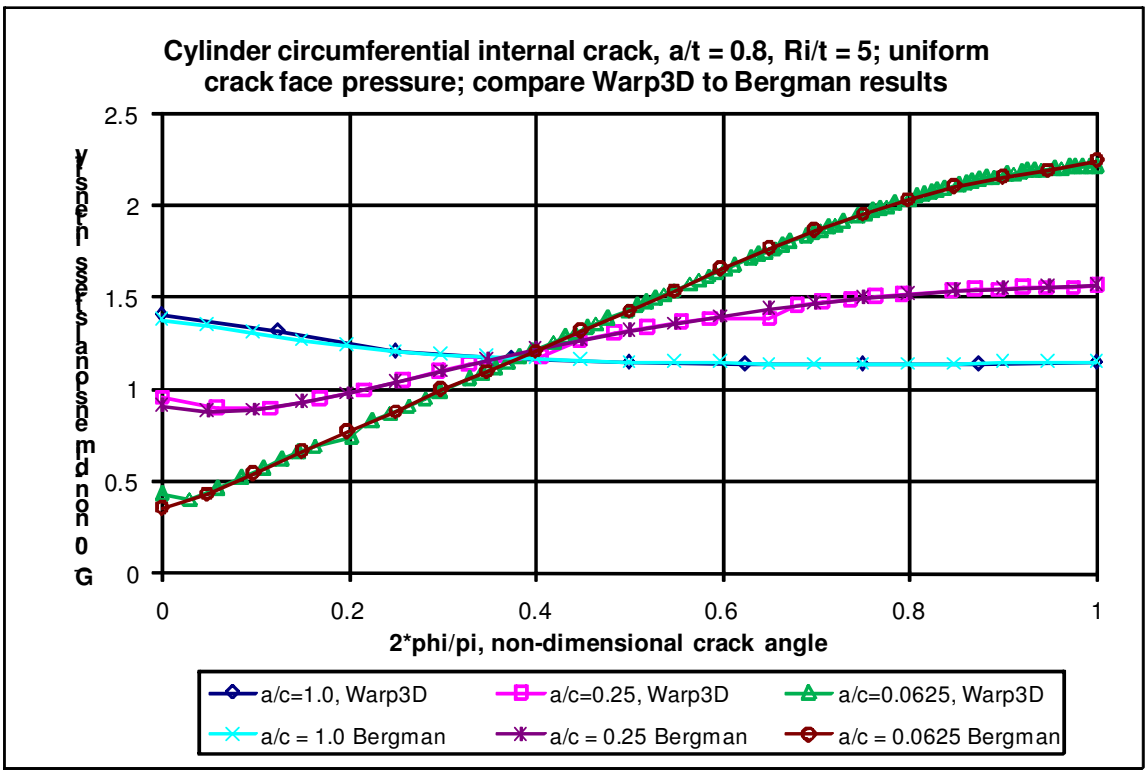

Figure 3-11. Compare G_0 results for the internal circumferential surface crack, a/t = 0.8, uniform crack face pressure

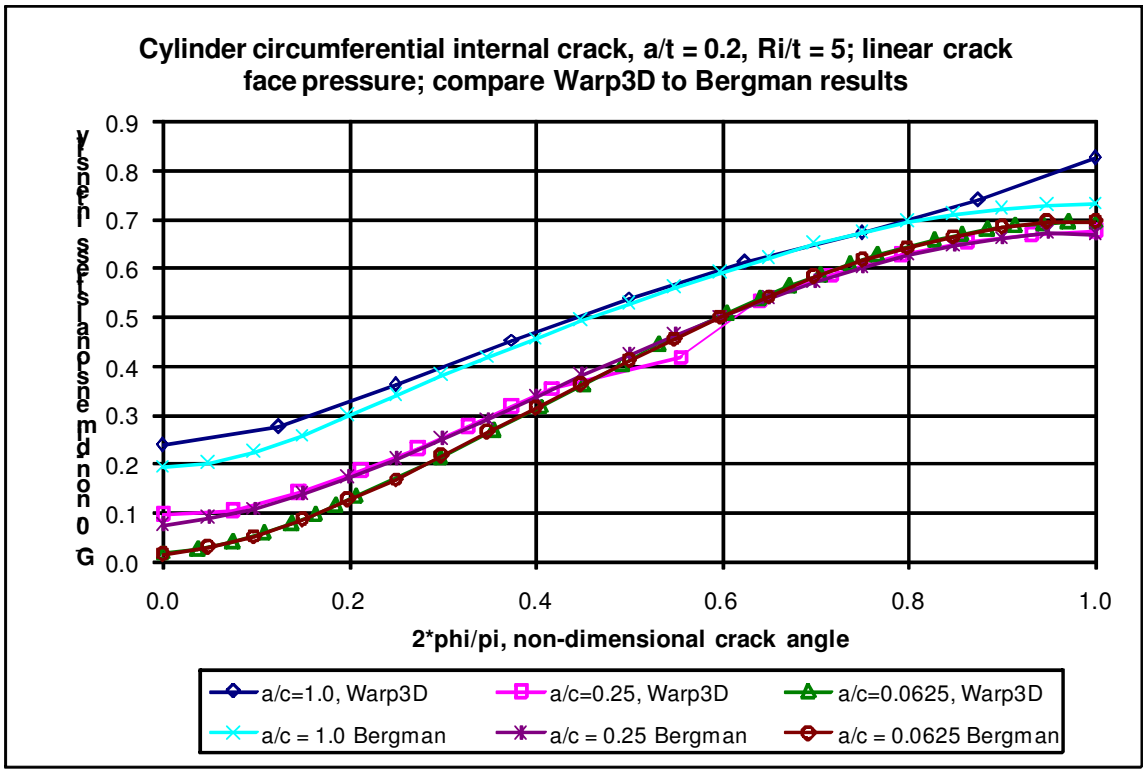

Figure 3-12. Compare G_0 results for the internal circumferential surface crack, a/t = 0.2, linear crack face pressure

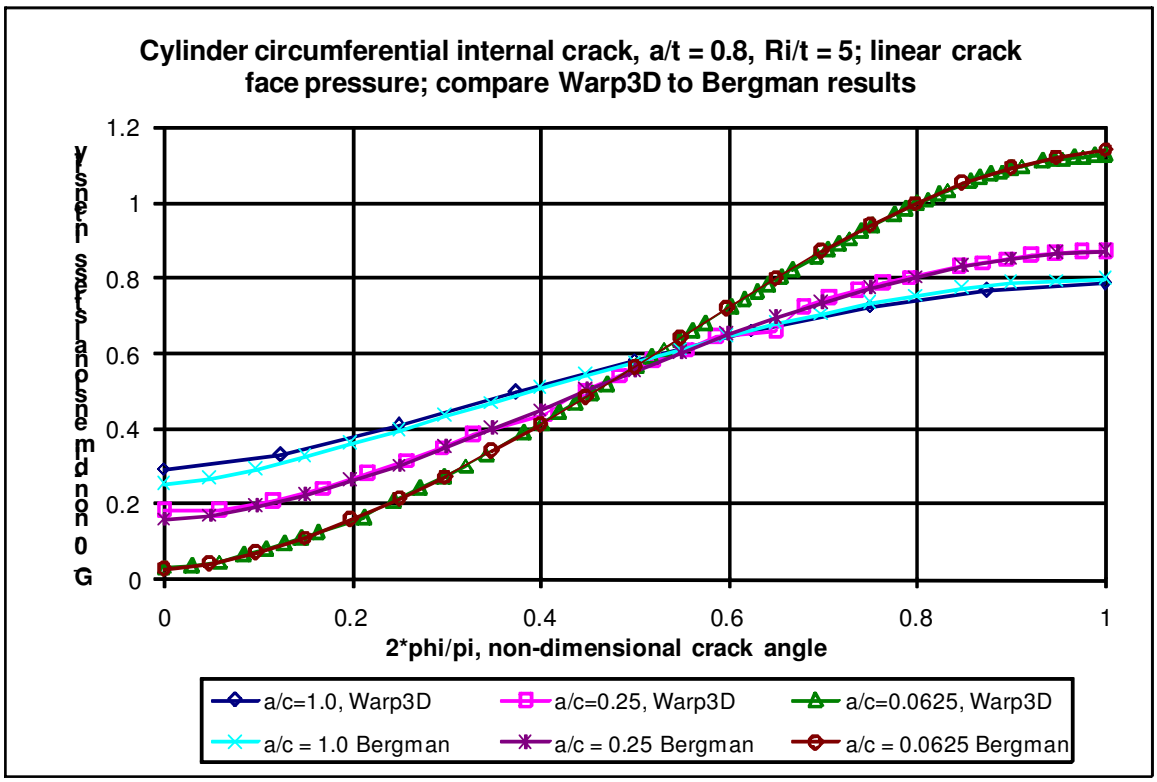

Figure 3-13. Compare G_0 results for the internal circumferential surface crack, a/t = 0.8, linear crack face pressure

Cylinder Surface Cracks ABAQUS Results

Groups of three *ABAQUS* crack mesh input files were generated by *FEACrack* for the cylinder internal circumferential surface crack aspect ratios *a/c* of 1.0, 0.25, and 0.0625. The crack depth ratio for each set of crack meshes *a/t* is 0.2 and 0.8. Uniform and linear crack face pressure loading is used for each set of crack meshes. The cylinder values used for these analyses are inside radius R_i of 5.0 in, thickness *t* of 1.0 in, cylinder length *L* of 15.0 in, and maximum crack face pressure magnitude *p* of 1000 psi. The material values used are Young's modulus of elasticity, *E*, of 30×10^6 psi, and Poisson's ratio, *v*, of 0.3. The comparison of the non-dimensional stress intensity results to the Bergman results is shown in Figures 3-14 through 3-17.

The FEA results from *ABAQUS* using the *FEACrack* crack meshes agree closely with the Bergman solutions. In most cases, the two sets of results are within 2% of one another. There is a somewhat greater difference, however, for the linear crack face pressure with *c/a* = 1 and *a/t* = 0.2 (Figure 3-16); the present results are approximately 5% higher than the Bergman results. The good results for the cylinder surface cracks verify that *FEACrack* is generating good crack meshes and that *ABAQUS* is computing the correct solution.

Convergence studies indicate that a relatively high degree of crack face mesh refinement is required to obtain accurate *K* solutions for non-uniform crack face pressure. If the mesh refinement is insufficient, the computed *K* values tend to *underestimate* the true solution. Since the present solution for *c/a* of 1 and *a/t* of 0.2 lies above the Bergman results, we believe the *FEACrack* crack mesh results are more reliable.

In some cases, the Bergman results and the present solutions differ by around 10% at the free surface ($\phi = 0$). J-integral estimates at the free surface tend to be unreliable and have higher path dependence in the contour integrals. For this reason, the free surface value is excluded when fitting the results to a 6^{th}-

order polynomial. We believe that this curve fit method produces better estimates of K at the free surface than estimates inferred directly from the computed J-integral at the crack tip.

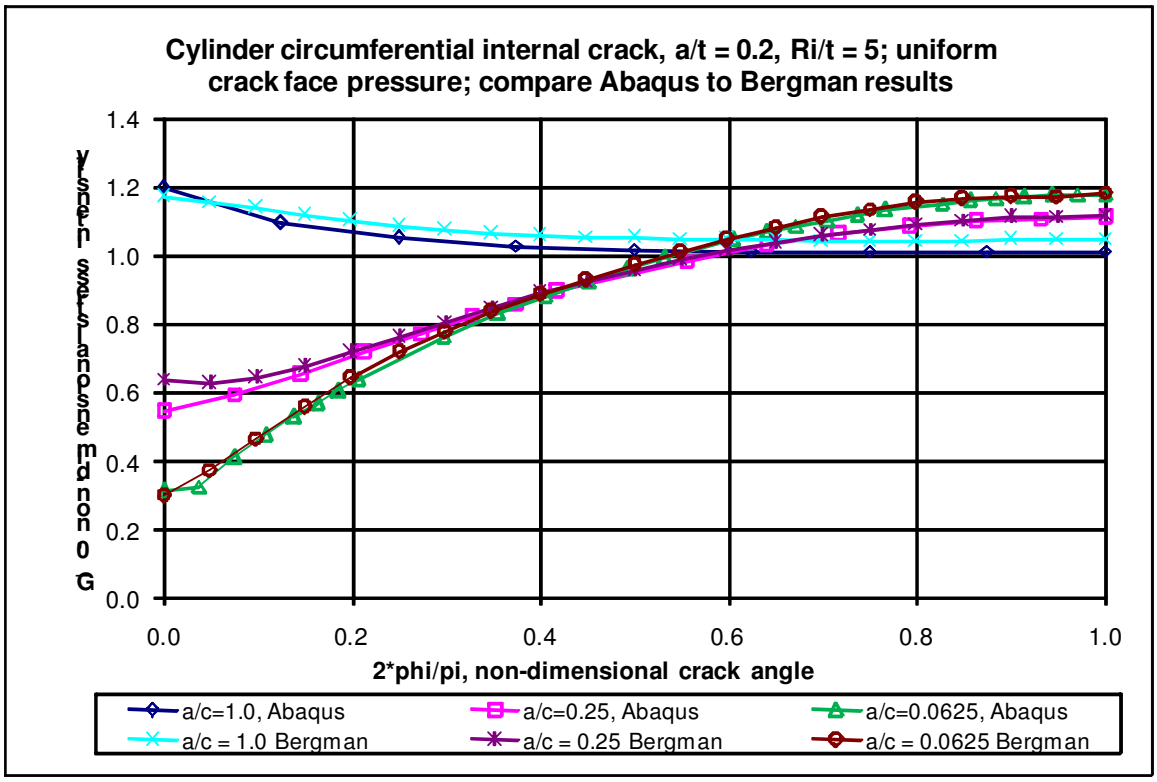

Figure 3-14. Compare G_0 results for the internal circumferential surface crack, a/t = 0.2, uniform crack face pressure

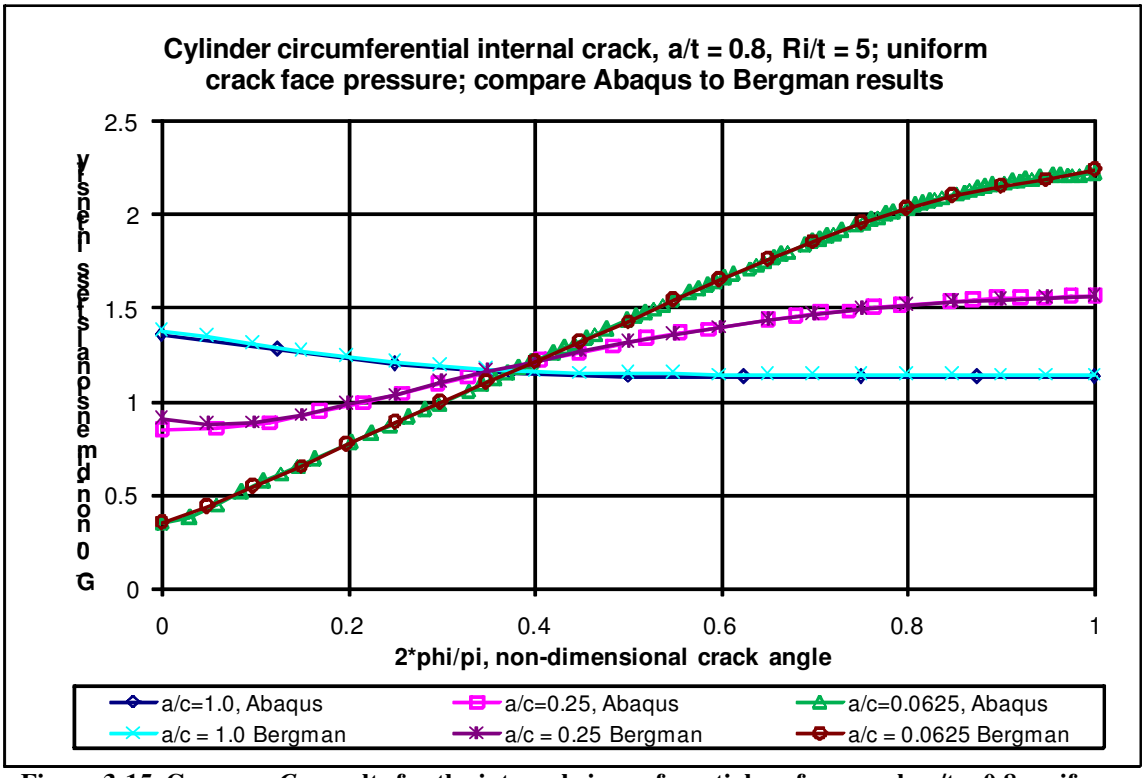

Figure 3-15. Compare G_0 results for the internal circumferential surface crack, a/t = 0.8, uniform crack face pressure

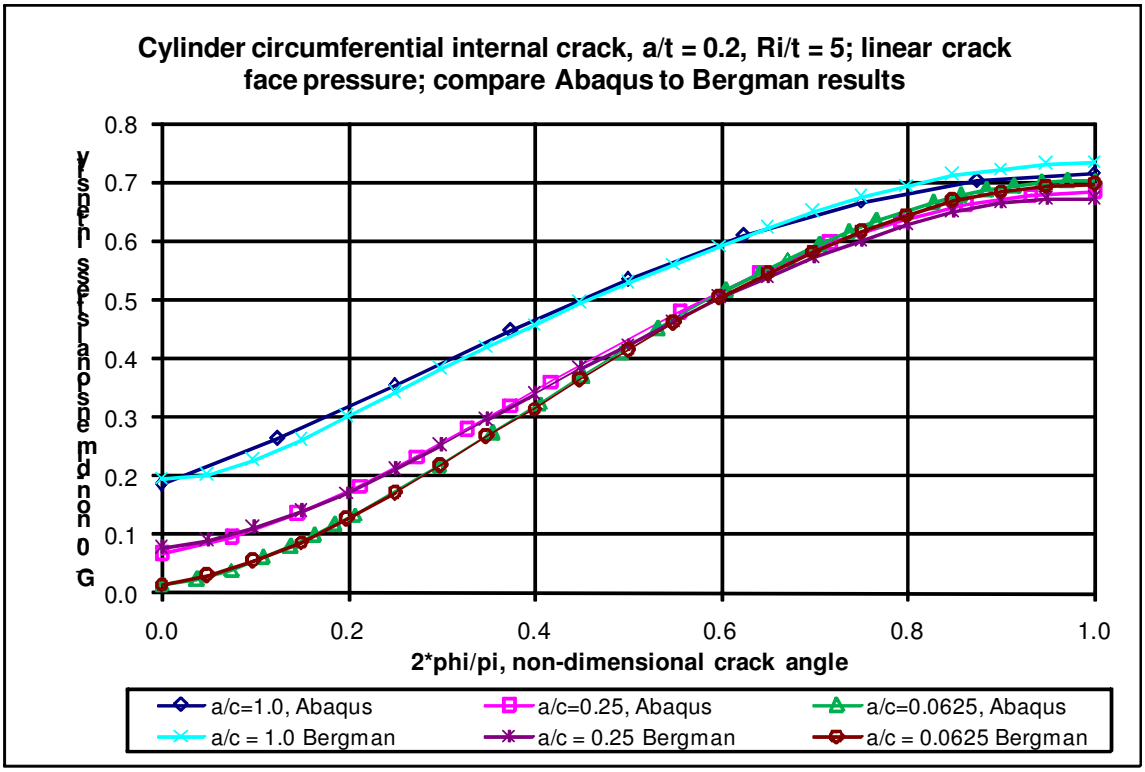

Figure 3-16. Compare G_0 results for the internal circumferential surface crack, a/t = 0.2, linear crack face pressure

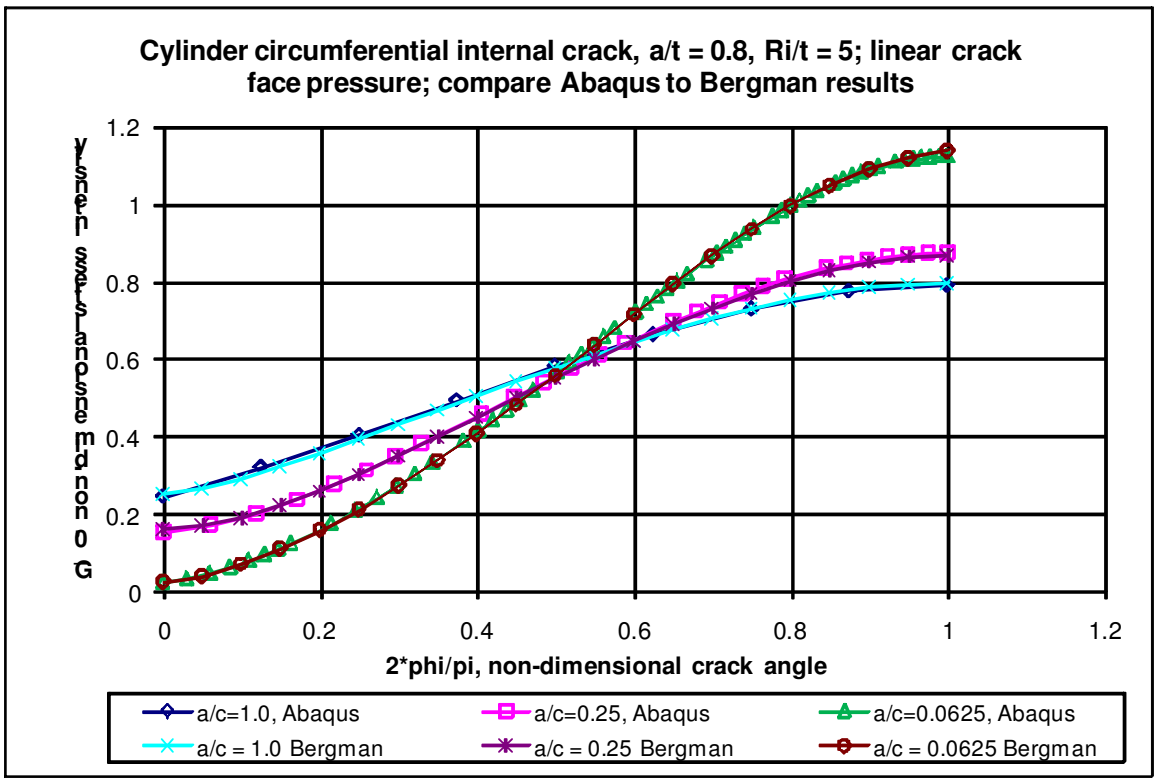

Figure 3-17. Compare G_0 results for the internal circumferential surface crack, a/t = 0.8, linear crack face pressure

Cylinder Surface Cracks ANSYS Results

As in the previous sections, groups of three *ANSYS* crack mesh input files were generated by *FEACrack* for the cylinder internal circumferential surface crack aspect ratios *a/c* of 1.0, 0.25, and 0.0625. The crack depth ratio for each set of crack meshes *a/t* is 0.2 and 0.8. Uniform and linear crack face pressure loading is used for each set of crack meshes. The cylinder values used for these analyses are inside radius R_i of 5.0 in, thickness *t* of 1.0 in, cylinder length *L* of 15.0 in, and maximum crack face pressure magnitude *p* of 1000 psi. The material values used are Young's modulus of elasticity, *E*, of 30×10^6 psi, and Poisson's ratio, *v*, of 0.3. The comparison of the non-dimensional stress intensity results to the Bergman results is shown in Figures 3-18 through 3-21.

The FEA results from *ANSYS* using the *FEACrack* crack meshes agree closely with the Bergman solutions; also refer to the additional discussion in the previous *ABAQUS* results section. The results verify that good crack meshes are being generated by *FEACrack* and the Quest Reliability J-integral module is computing correct values using *ANSYS* results.

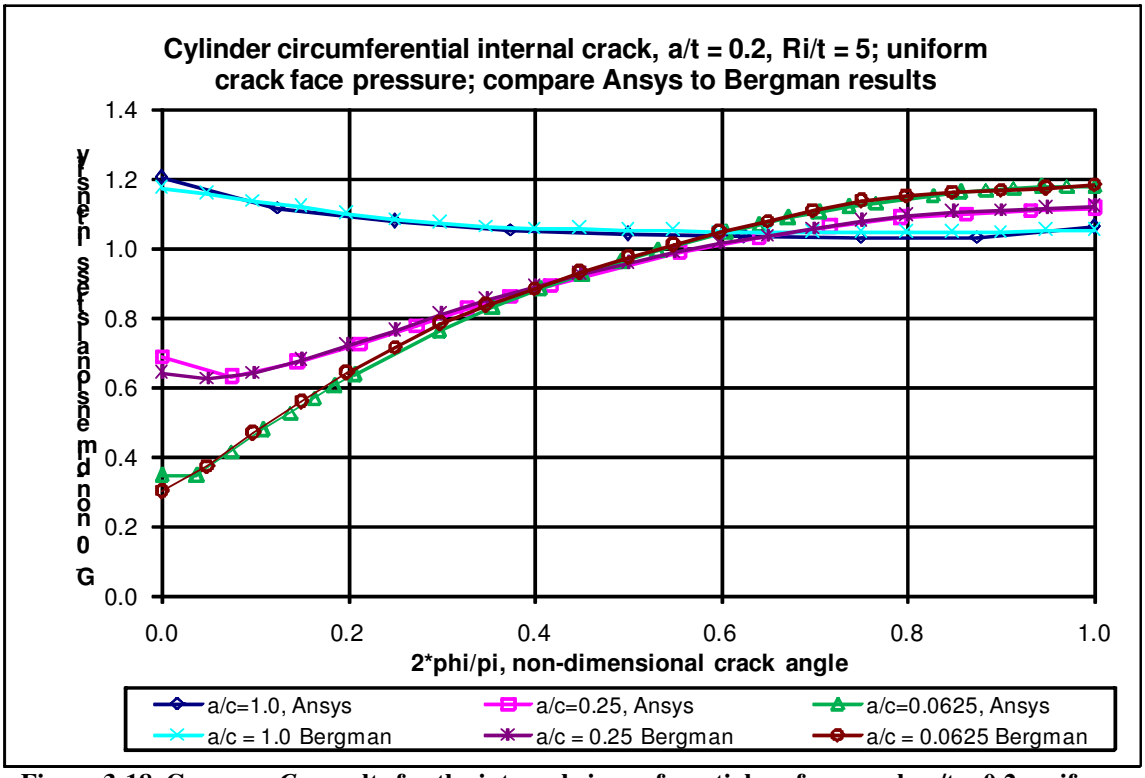

Figure 3-18. Compare G_0 results for the internal circumferential surface crack, a/t = 0.2, uniform crack face pressure

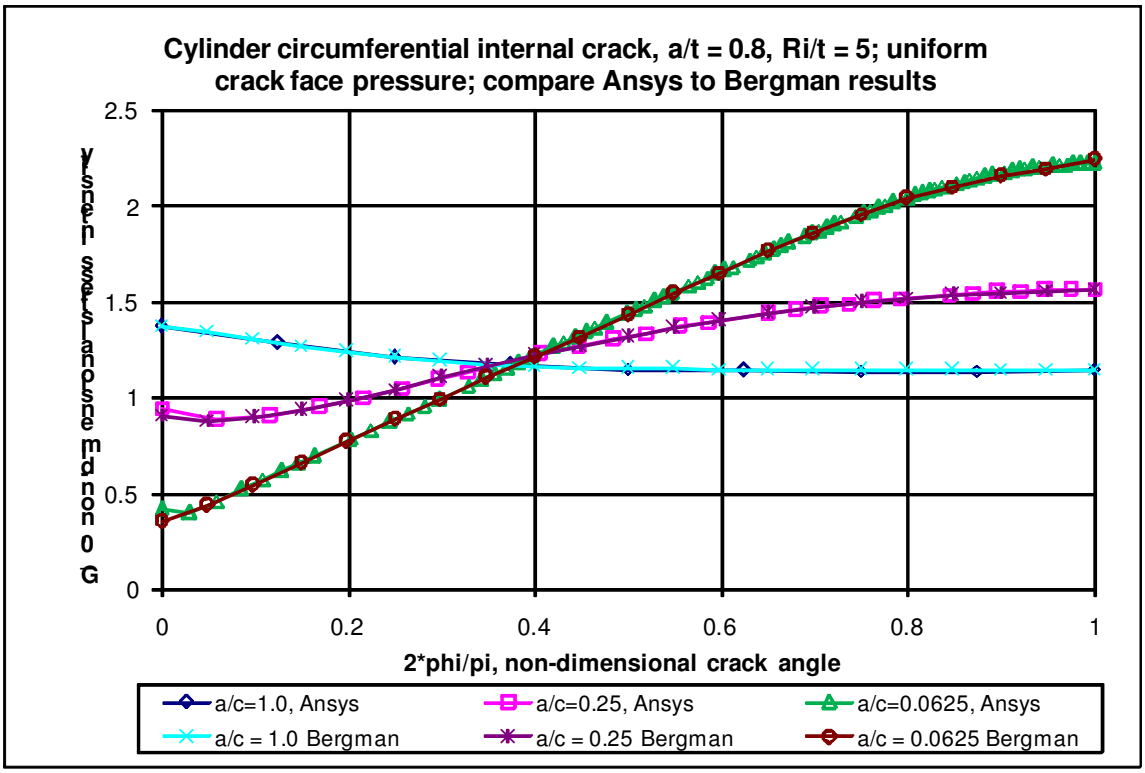

Figure 3-19. Compare G_0 results for the internal circumferential surface crack, a/t = 0.8, uniform crack face pressure

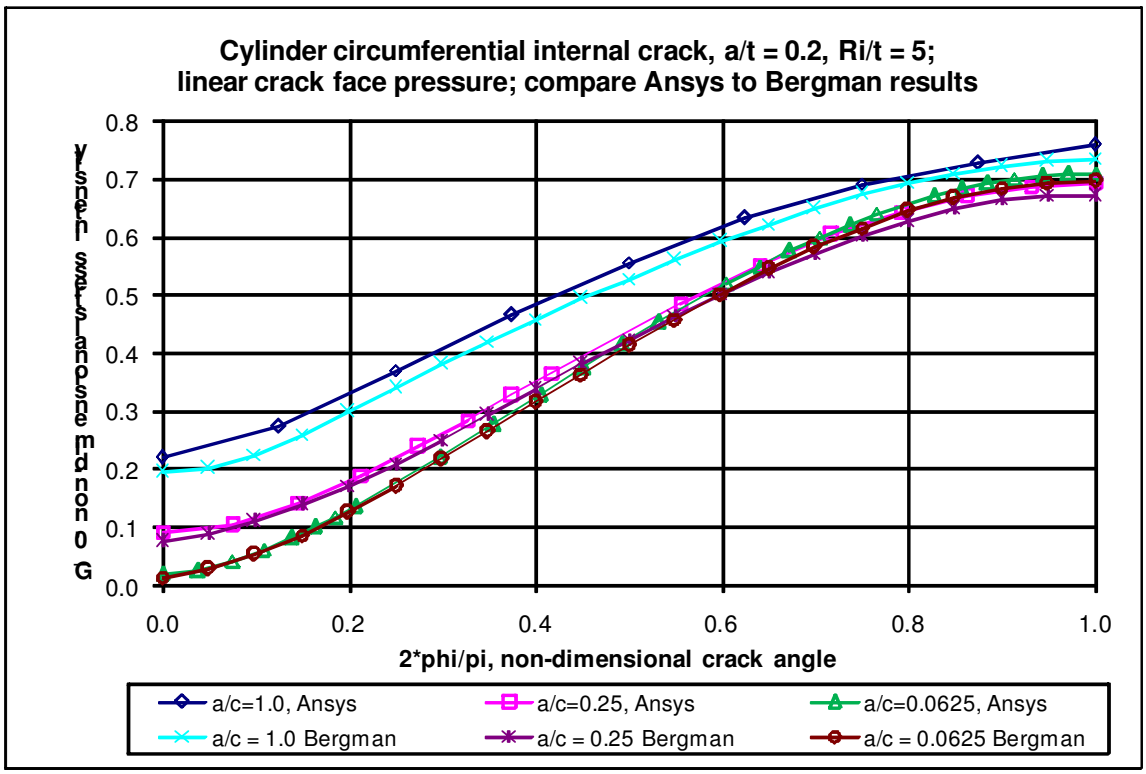

Figure 3-20. Compare G_0 results for the internal circumferential surface crack, a/t = 0.2, linear crack face pressure

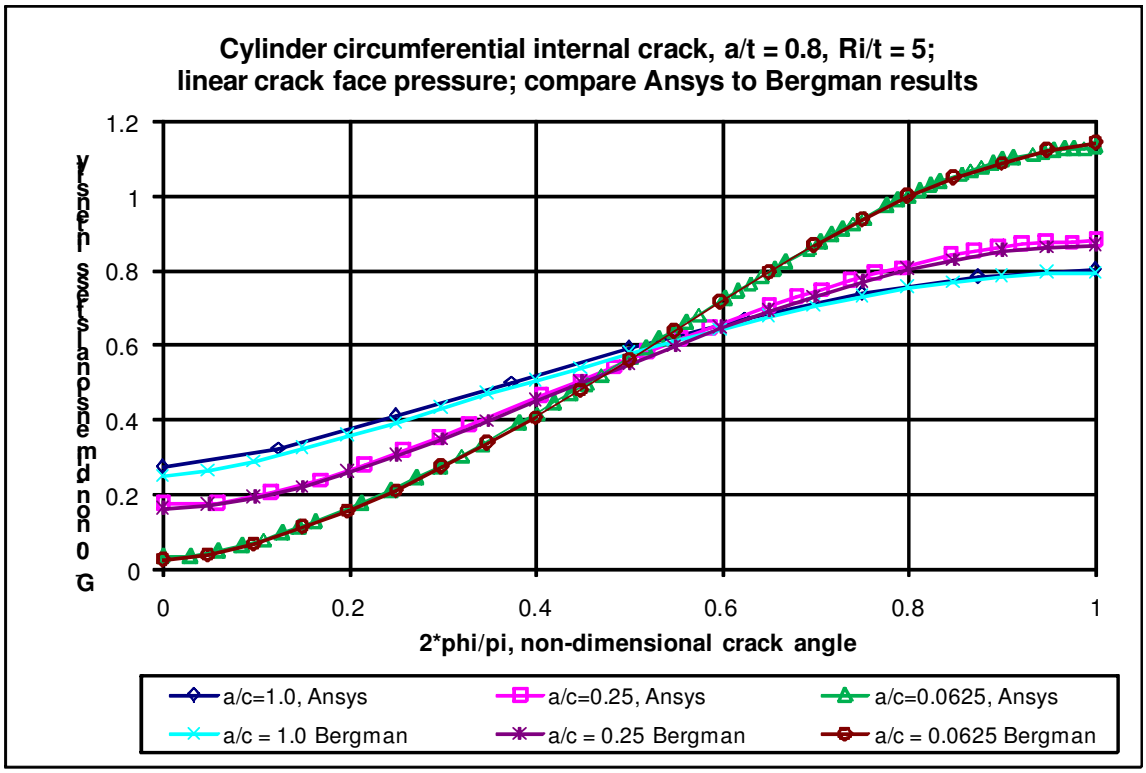

Figure 3-21. Compare G_0 results for the internal circumferential surface crack, a/t = 0.8, linear crack face pressure

Through Thickness Crack

An infinite plate with a through thickness crack has a closed form stress intensity solution [3] given by:

$$K_I = \sigma\sqrt{\pi c} \tag{4.1}$$

Where σ is the remote stress applied perpendicular to the crack plane for mode I crack opening, and c is the through crack half-length (full crack length is $2c$), see Figure 4-1.

FEACrack was used to generate a set of quarter symmetric crack meshes with increasing crack length; a typical through crack mesh is shown in Figure 4-2. Appropriate mesh constraints for symmetry were applied to the left and front mesh surfaces. Since the plate must have a finite size for the finite element analysis, the plate width and length dimensions are large compared to the crack length so that mesh boundary effects in the J-integral results are negligible. The crack lengths analyzed were c of 0.5, 1, 2, 4, and 8 in ($2c$ is entered in *FEACrack*). The plate dimensions for the first four meshes were thickness t of 1 in, plate half width W and plate half length L of 40 in. For the longest crack length the plate half width and plate half length were increased to 80 in. The Young's modulus of elasticity, E, was 30×10^6 psi. The first set of analyses was computed with a Poisson ratio, ν, of zero to remove 3-D through thickness effects to better model the infinite plate and remove any out of plane effects in the FEA solution. The second set of analyses used a typical Poisson's ratio of 0.3 to model the through crack in a 3D plate and observe 3D effects in the crack results. FEA results are compared to theory in the following sections.

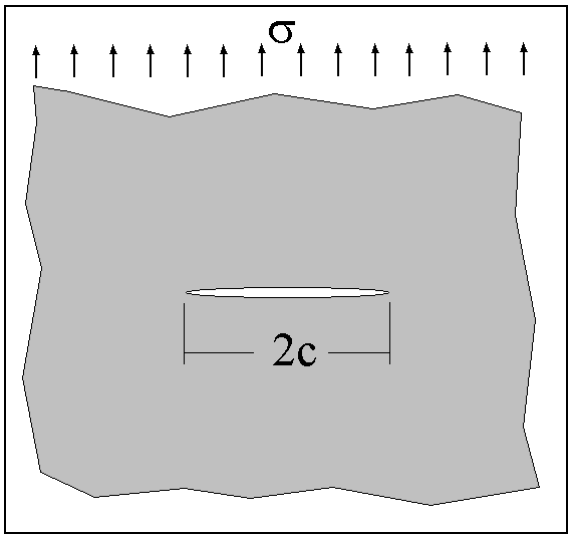

Figure 4-1. Through thickness crack in an infinite plate; the remote stress is normal to the crack direction

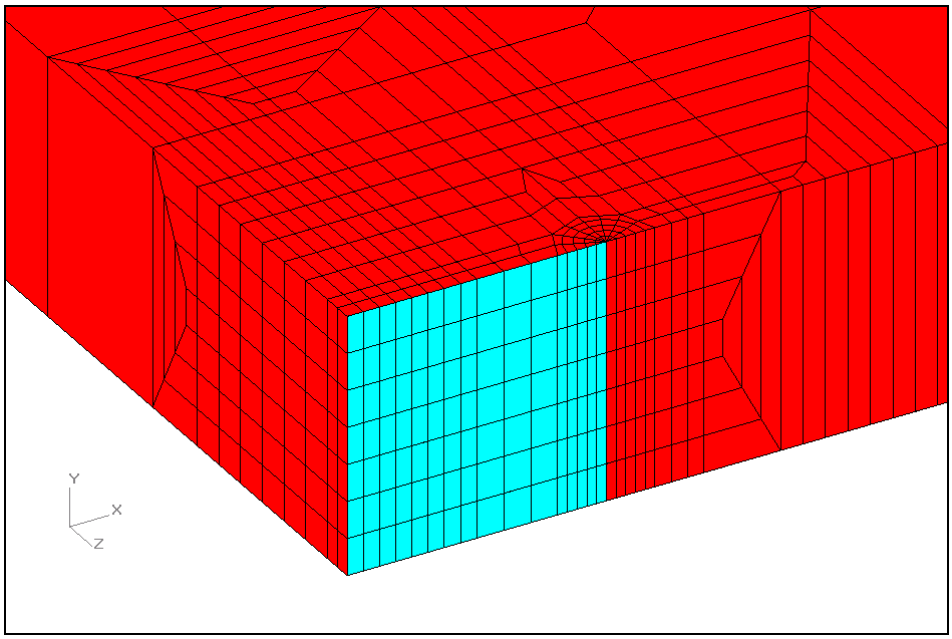

Figure 4-2. Through thickness crack mesh, 2c = 2 in, thickness = 1 in

Through Crack WARP3D Results

The through thickness crack mesh *WARP3D* results using a Poisson ratio of zero compare very closely to the theoretical solution for each crack length, typically within one percent or less, see Figure 4-3. Both the stress intensity *K* computed from the J-integral and the *K* computed from the crack opening displacement agrees closely with the theoretical solution. These results verify that a good through-thickness crack mesh is being generated by *FEACrack* and that the *WARP3D* program is computing the results correctly.

When the Poisson ratio of 0.3 is used for a through crack in a 3-D plate, 3-D effects along the crack front appear in the results, see Figure 4-4. The *K* values at *y/t* of 0 and 1 are close from both sets of analyses (Poisson ratio of 0 and 0.3), but when the Poisson ratio is 0.3 the *K* results increase toward the center of the plate thickness showing the effect of the finite plate thickness.

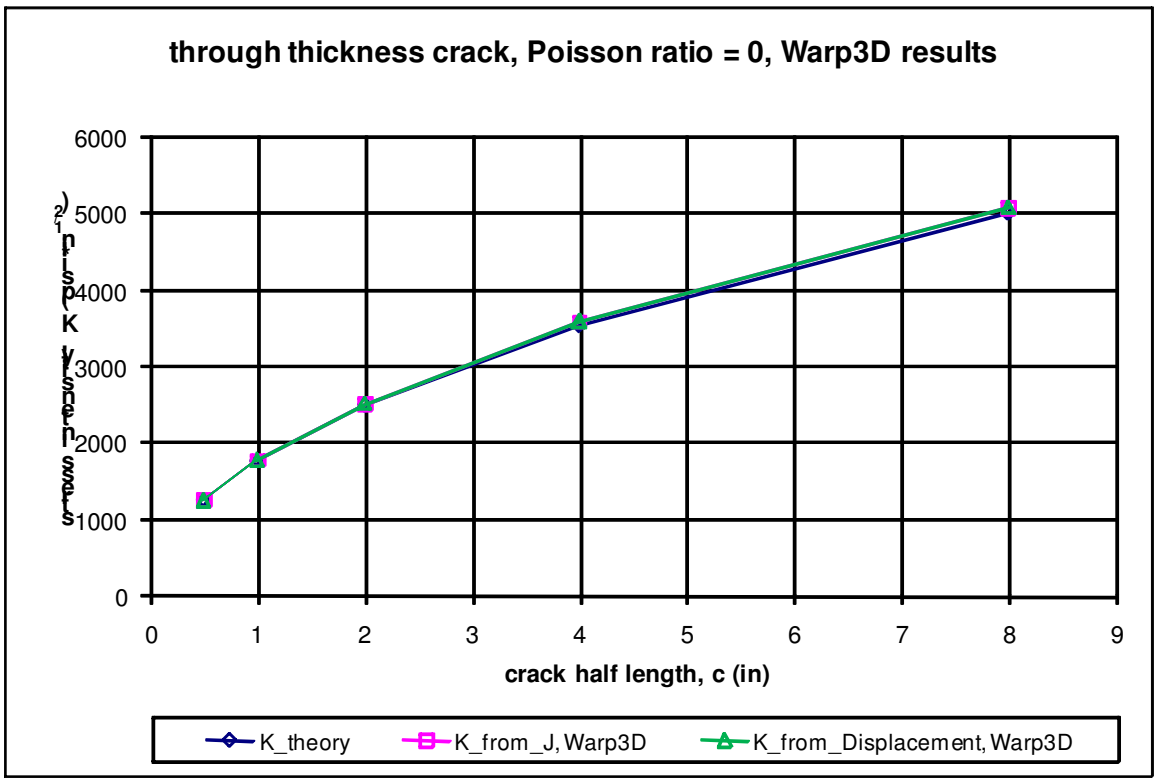

Figure 4-3. Through thickness crack results comparison to theory, Poisson ratio set to zero

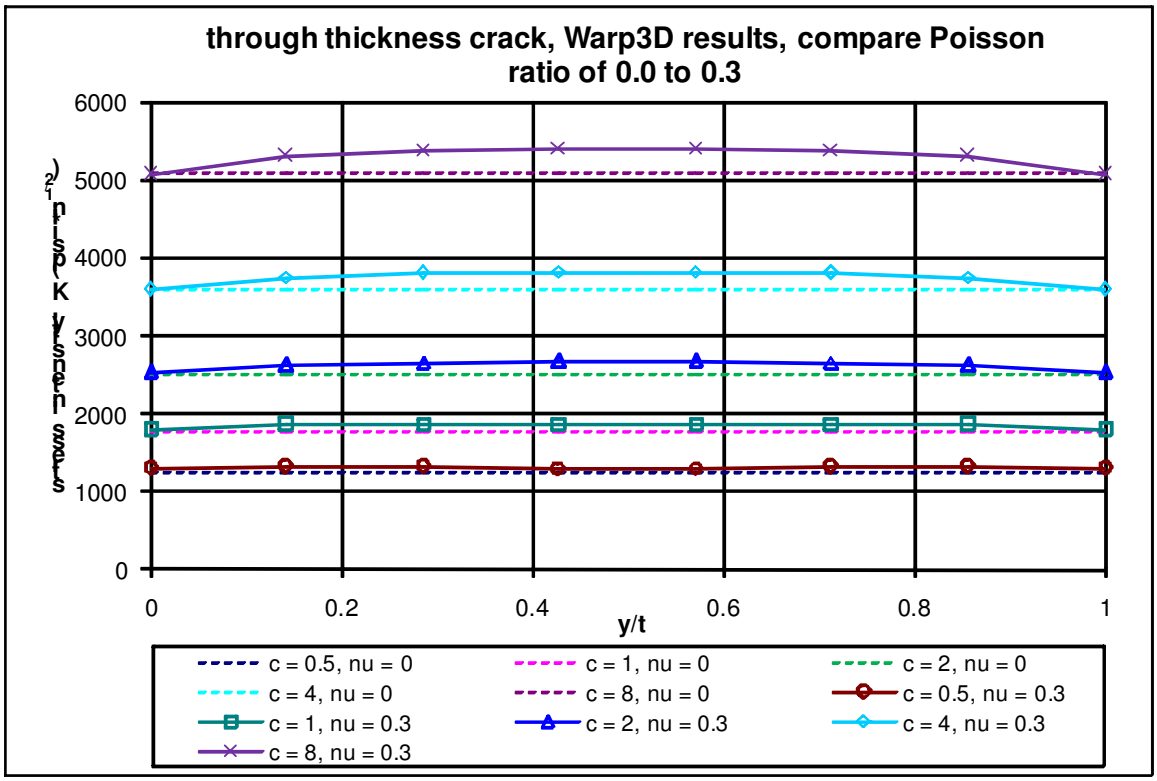

Figure 4-4. Through thickness crack results along the crack front for two values of Poisson ratio

Through Crack ABAQUS Results

The through thickness crack mesh *ABAQUS* results using a Poisson ratio of zero compare very closely to the theoretical solution for each crack length, typically within one percent or less, see Figure 4-5. Both the stress intensity *K* computed from the J-integral and the *K* computed from the crack opening displacement agree closely with the theoretical solution. These results verify that a good through-thickness crack mesh is being generated by *FEACrack* and that the *ABAQUS* program is computing the results correctly.

When the Poisson ratio of 0.3 is used for a through crack in a 3-D plate, 3-D effects along the crack front appear in the results, see Figure 4-6. When the Poisson ratio is 0.3 the *K* results increase toward the center of the plate thickness showing the effect of the finite plate thickness.

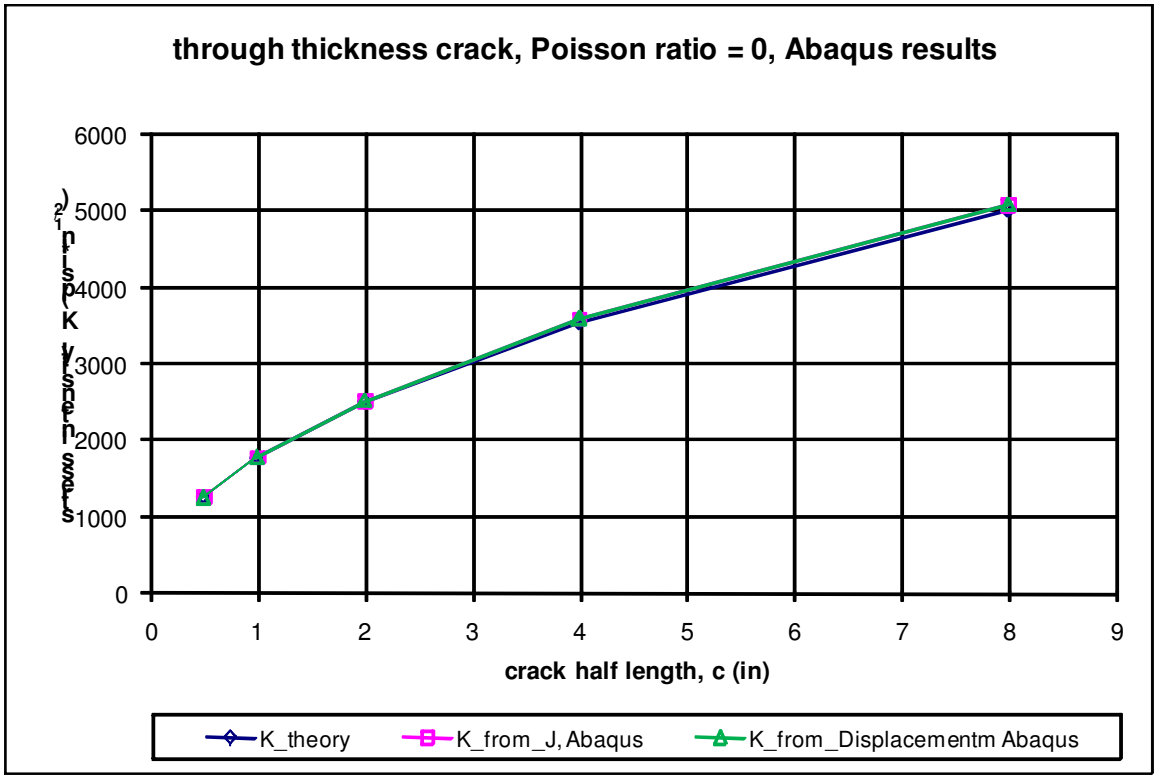

Figure 4-5. Through thickness crack results comparison to theory, Poisson ratio set to zero

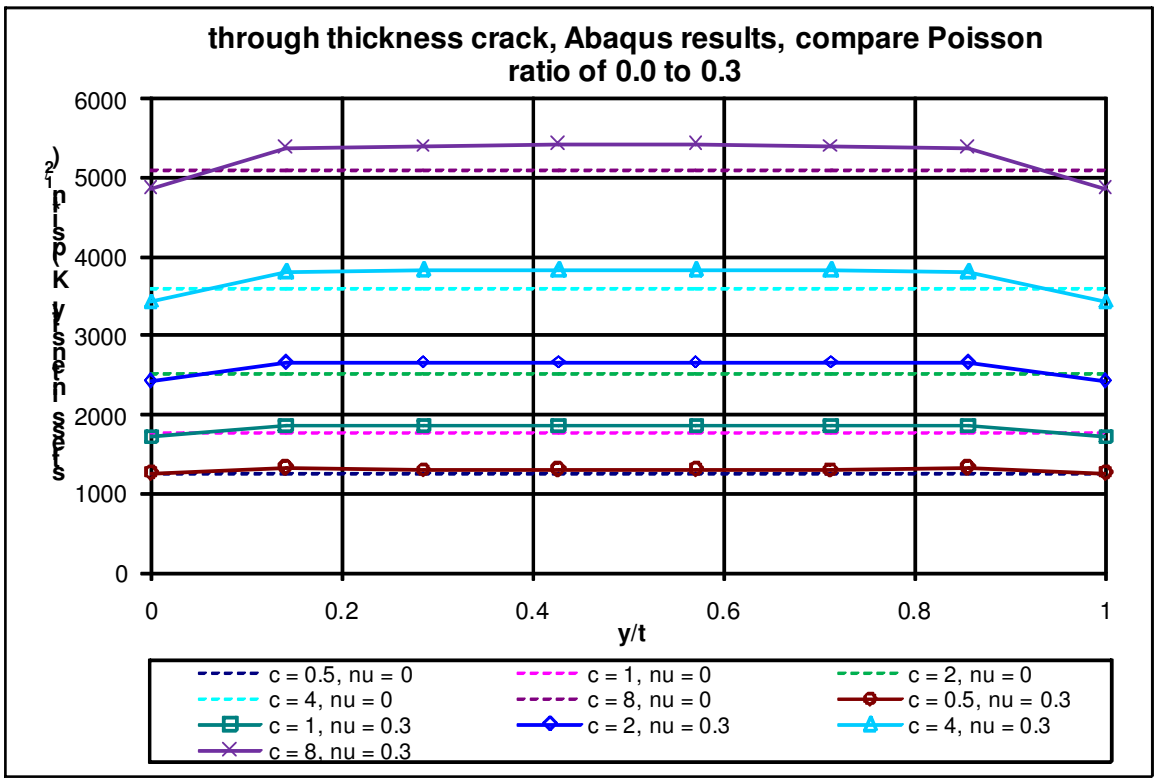

Figure 4-6. Through thickness crack results along the crack front for two values of Poisson ratio

Through Crack ANSYS Results

The through thickness crack mesh *ANSYS* results using a Poisson ratio of zero compare very closely to the theoretical solution for each crack length, typically within one percent or less, see Figure 4-7. Both the stress intensity *K* computed from the J-integral and the *K* computed from the crack opening displacement agrees closely with the theoretical solution. These results verify that a good through thickness crack mesh is being generated by *FEACrack* and that the *ANSYS* program and the Quest Reliability J-integral module are computing the results correctly.

When the Poisson ratio of 0.3 is used for a through crack in a 3-D plate, 3-D effects along the crack front appear in the results, see Figure 4-8. The *K* values at *y/t* of 0 and 1 are close from both sets of analyses (Poisson ratio of 0 and 0.3), but when the Poisson ratio is 0.3 the *K* results increase toward the center of the plate thickness showing the effect of the finite plate thickness.

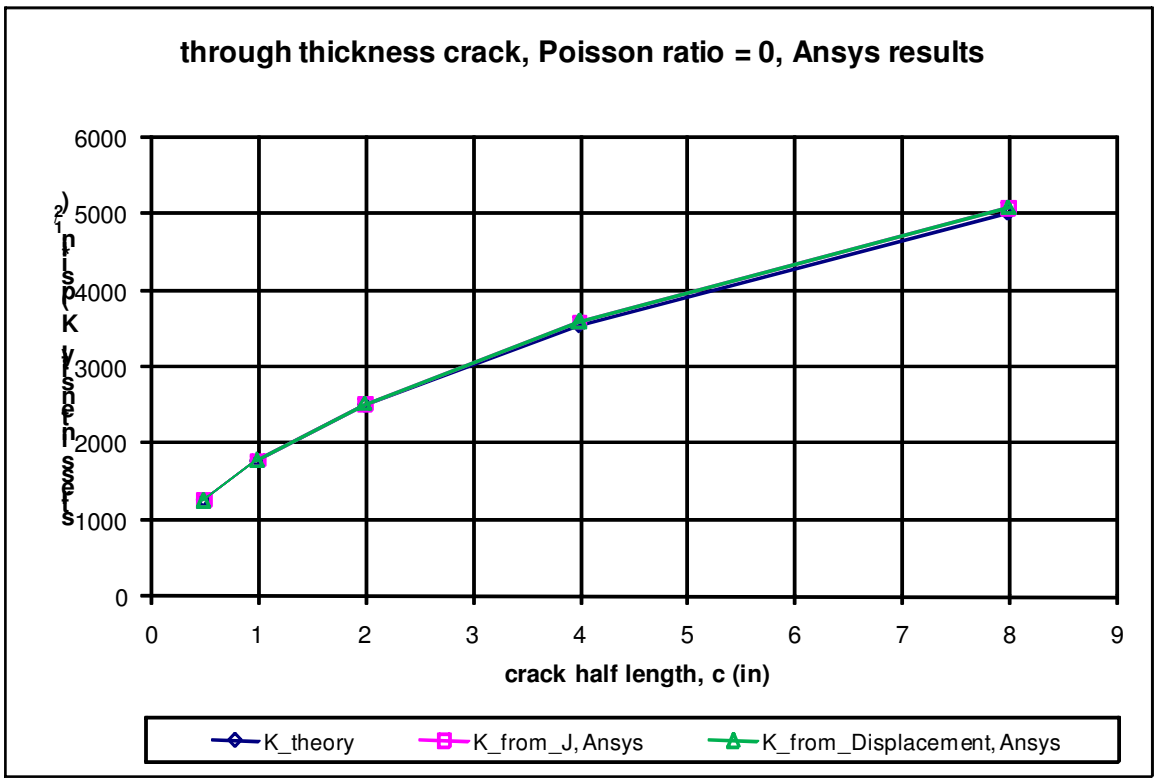

Figure 4-7. Through thickness crack results comparison to theory, Poisson ratio set to zero

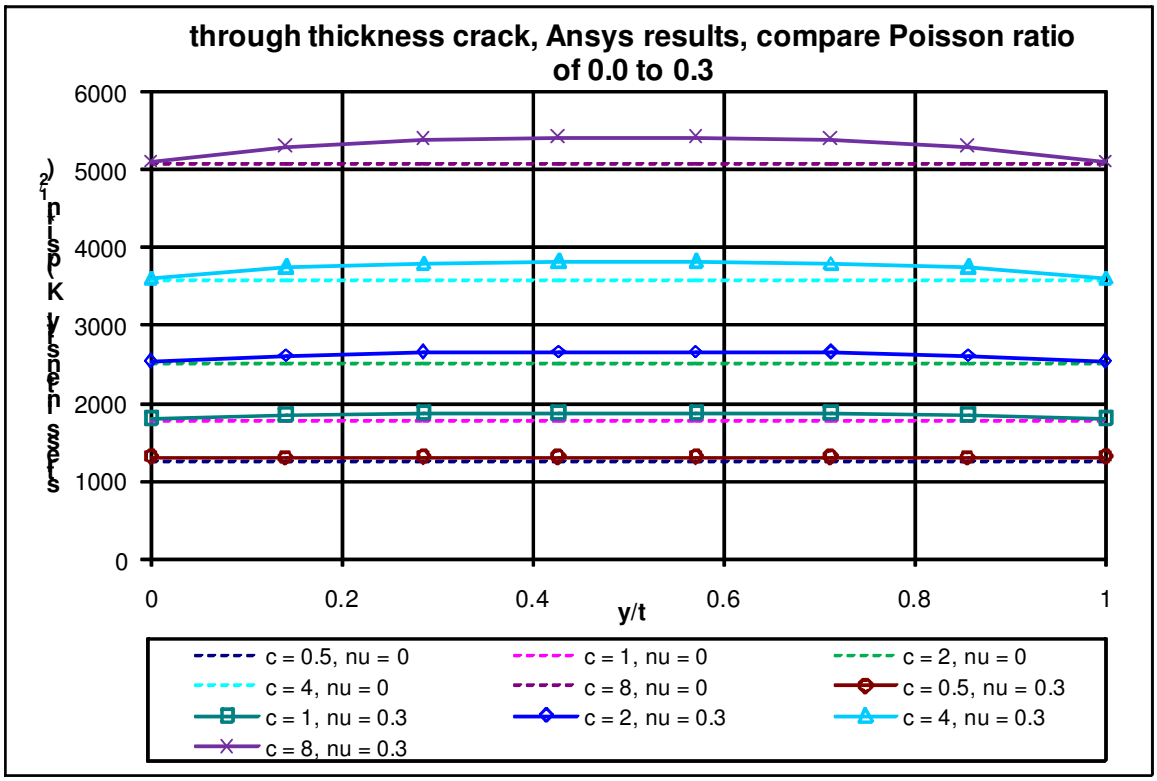

Figure 4-8. Through thickness crack results along the crack front for two values of Poisson ratio

Full Plate with Surface Crack

The crack meshes in previous sections have used symmetry planes in the geometry and crack plane. Using symmetry reduces the mesh size giving quicker analyses; the crack plane can also be more easily viewed. In some cases there will not be a symmetry plane through the crack so the full mesh must be generated. A full plate mesh with the full surface crack is used to compare results between the FEA programs. In Figure 5-1 the full plate mesh is shown with the surface crack at the center of the plate; the crack tips at the right end of the crack ($\phi = 0$) and at the left end of the crack ($\phi = \pi$) are visible by their focused mesh pattern. The flat plate mesh width and length are 6 in, the plate thickness is 1 in, the applied remote stress, σ_z, is 5000 psi. The surface crack depth a is 0.5 in, and the surface crack length $2c$ is 1 in. The Young's modulus of elasticity is 30×10^6 psi, and the Poisson ratio is 0.3.

Results from each FEA program are compared in Figures 5-2 through 5-5. The stress intensity K results from the J-integral and from the crack opening displacement are compared to verify the crack results. The K-from-J and K-from-displacement results are typically within 2%. In Figure 5-5 the K-from-J results from each FEA program are compared for the flat plate. The close agreement verifies that each FEA program is computing the correct solution for the full surface crack mesh.

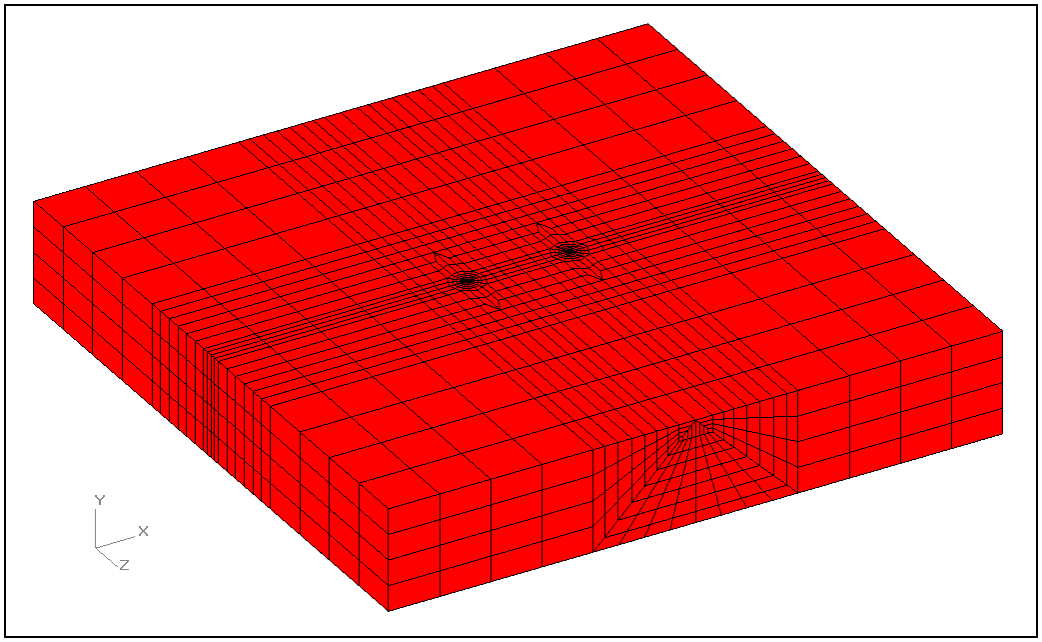

Figure 5-1. Full plate mesh with a full surface crack; the crack is located in the center of the plate.

In Figure 5-2 the FEA K results are slightly higher than the theoretical K solution. This is due to the crack depth a/t=0.5 showing the effect of the finite size plate in comparison to the infinite size plate for the theoretical solution. In Figure 5-7 the shallow crack a/t=0.1 results show a very good comparison between the theoretical solution and the FEA K results. The crack is shallow enough to avoid an effect from the finite size plate mesh.

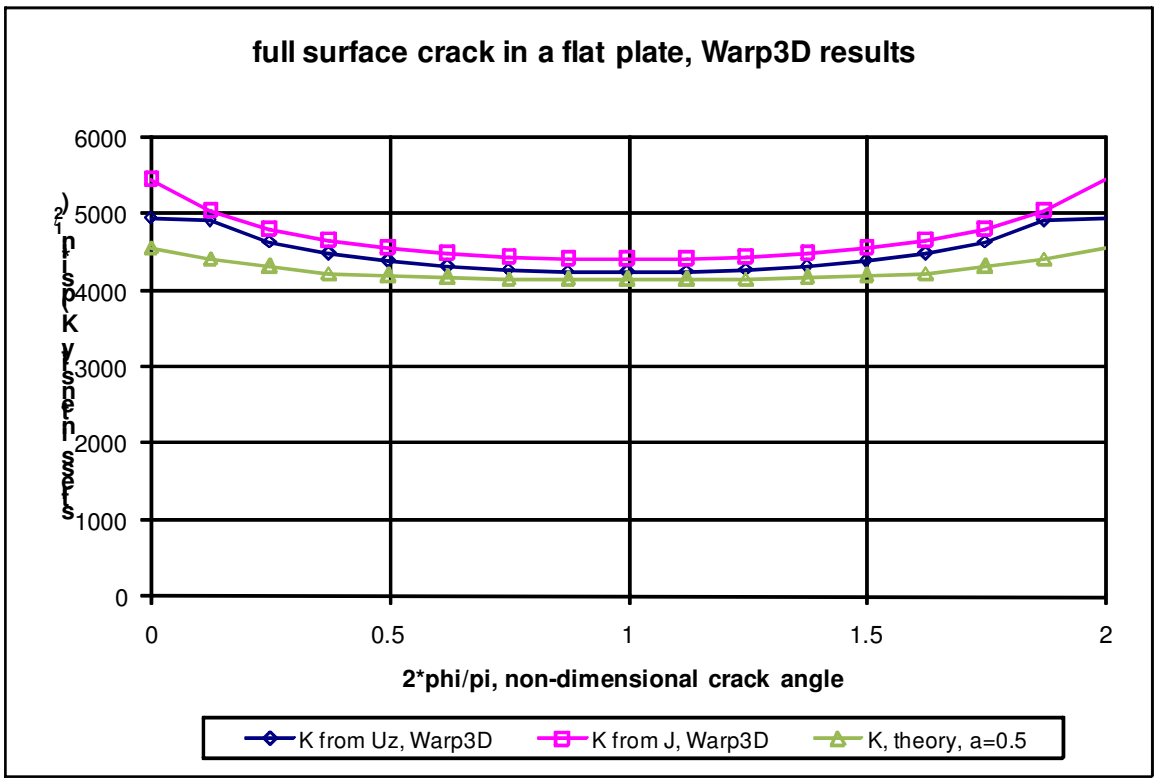

Figure 5-2. Compare *WARP3D K* results for the full plate with surface crack, a/t=0.5.

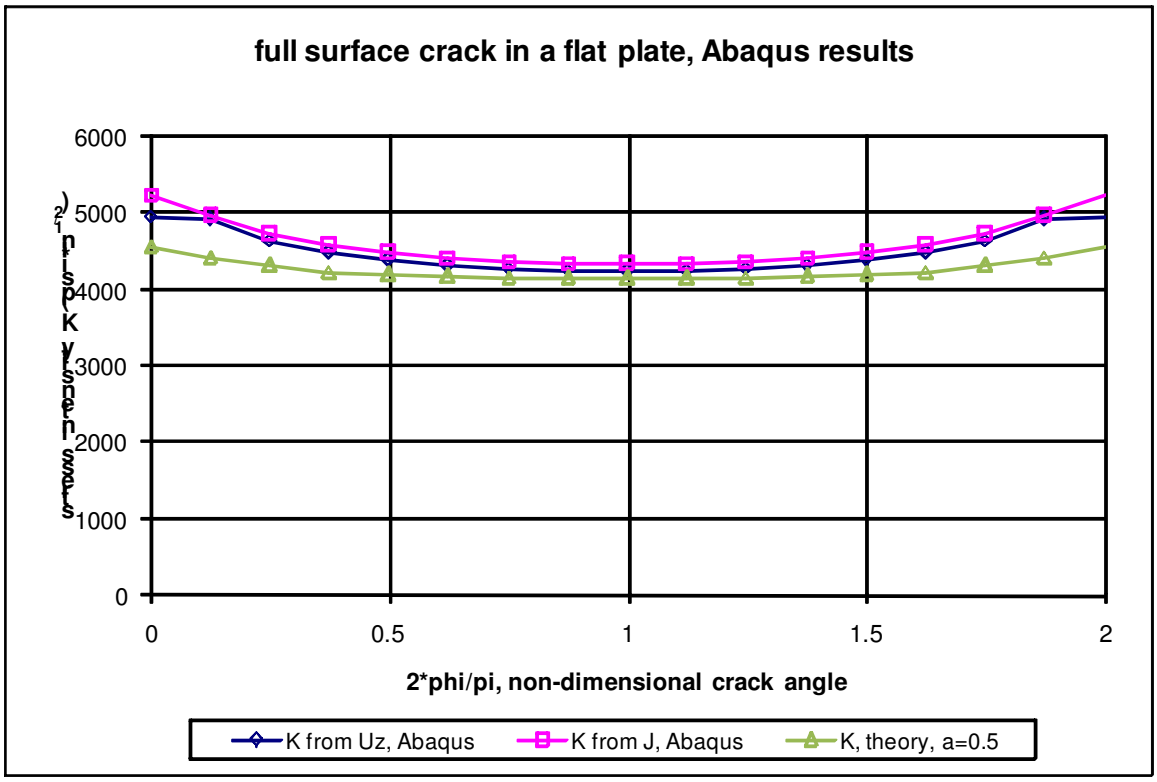

Figure 5-3. Compare *ABAQUS K* results for the full plate with surface crack.

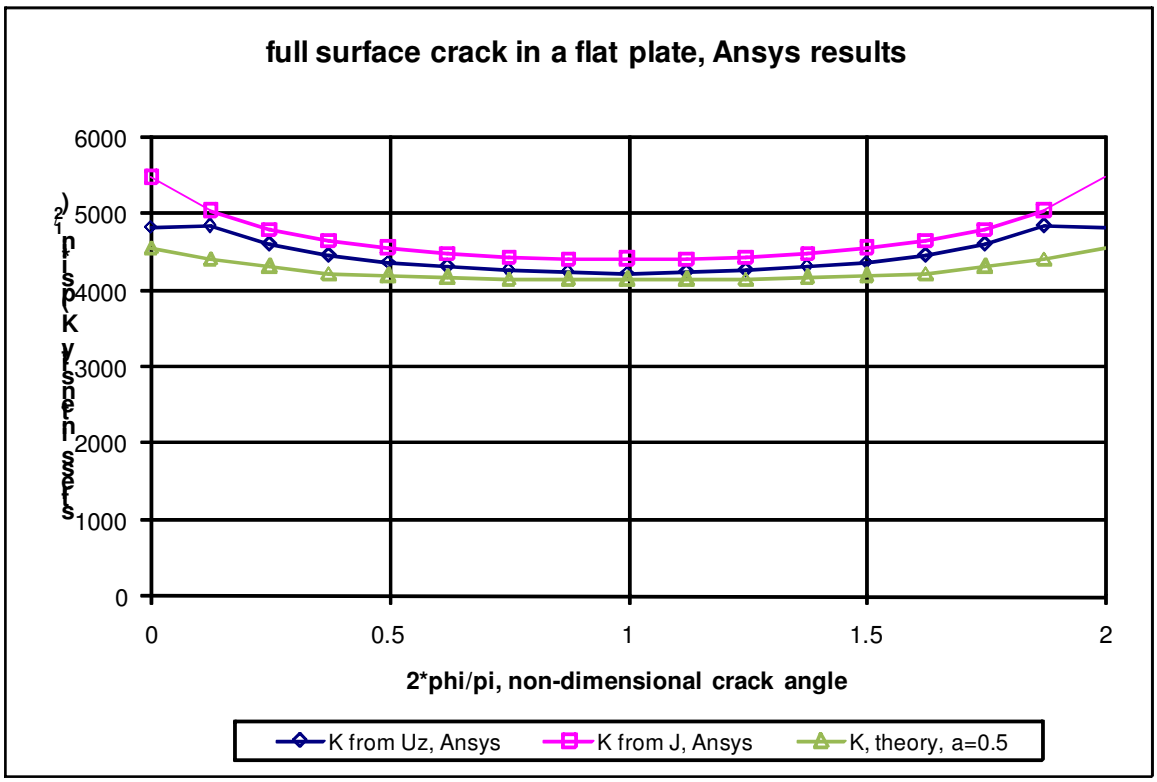

Figure 5-4. Compare *ANSYS K* results for the full plate with surface crack.

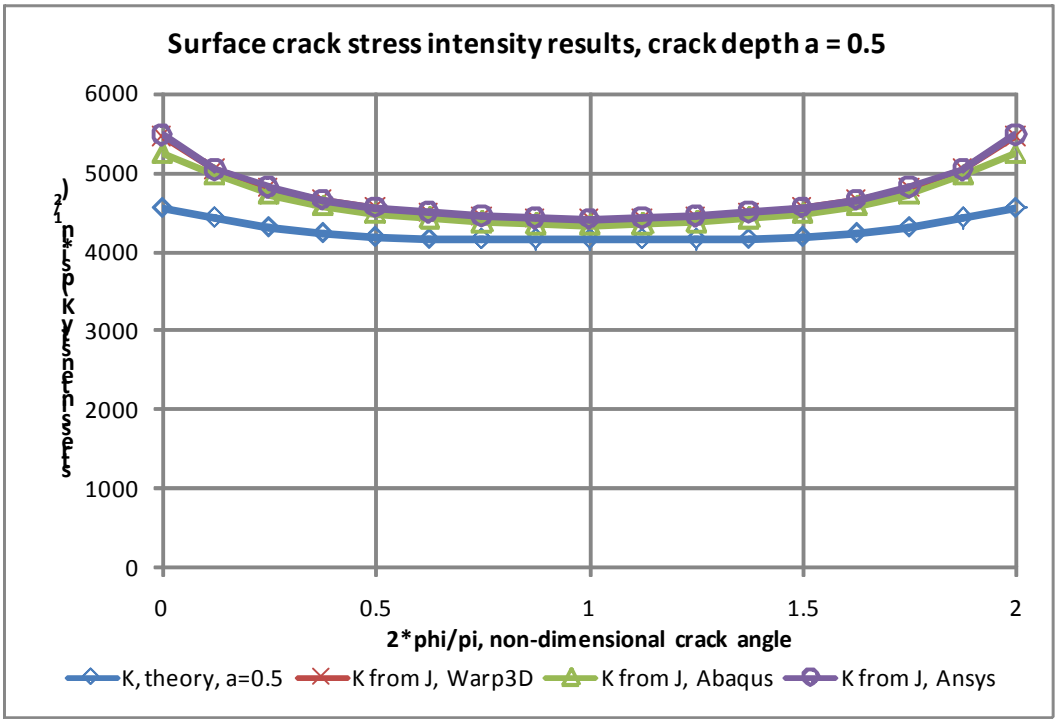

Figure 5-5. Compare *K* results from each FEA program to theory for the full plate with surface crack, a = 0.5.

Shallow Surface Crack

A shallow crack mesh is also available in *FEACrack*. The crack mesh is built in a smaller primitive to give a good mesh around the crack and the crack mesh pattern is extruded around the crack mesh to complete the given dimensions. Figure 5-6 shows a shallow crack in the center of the flat plate. The flat plate mesh width and length are 2 in, the plate thickness is 1 in, the applied remote stress, σ_z, is 5000 psi. The surface crack depth *a* is 0.1 in giving a crack depth ratio *a/t* of 0.1, and the surface crack length 2*c* is 0.2 in. The Young's modulus of elasticity is 30×10^6 psi, and the Poisson ratio is 0.3.

In Figure 5-7 the K-from-J results from each FEA program are compared. The shallow crack results match very closely from each FEA program and to the theoretical solution verifying that each program is computing the correct results for the shallow crack mesh.

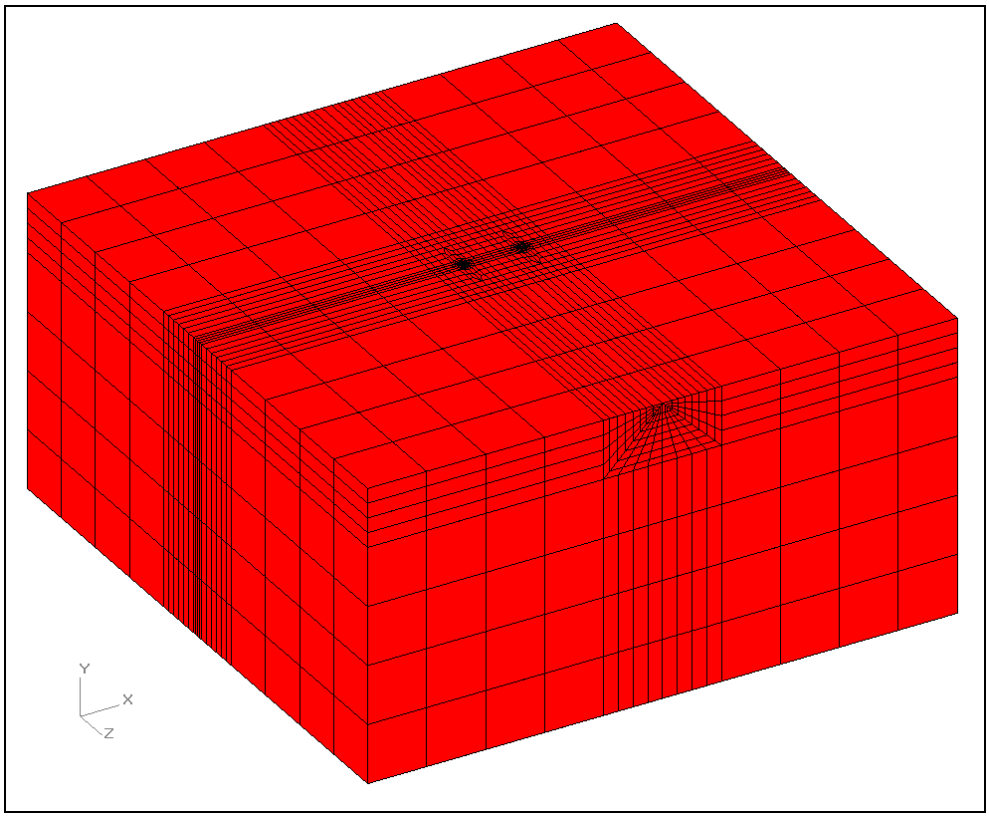

Figure 5-6. Shallow surface crack in a full plate mesh; the crack is located in the center of the plate.

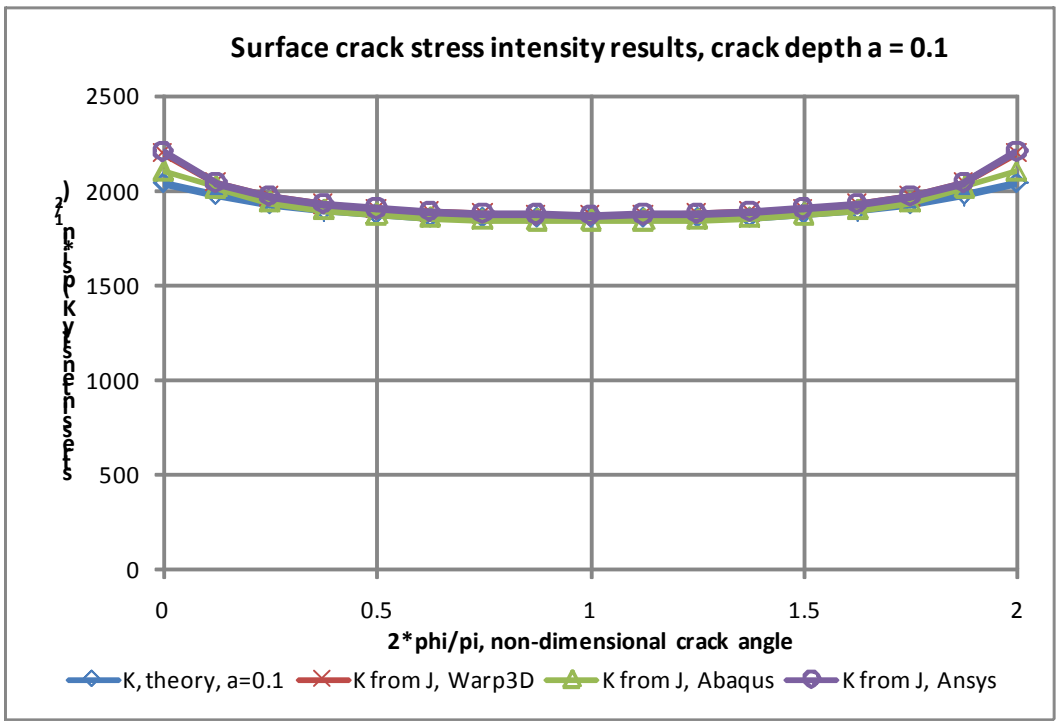

Figure 5-7. Compare *K* results from each FEA program for the shallow surface crack, a = 0.1.

Nozzle with Surface Crack

A more complex geometry is a nozzle on a shell (the intersection of two cylinders or pipes) with the crack at the toe of the fillet weld. Figure 6-1 shows the right half symmetric nozzle crack mesh, and Figure 6-2 shows a close-up of the surface crack and the fillet weld. The top of the crack ($\phi = 0$) and the deepest point of the crack on the symmetry plane ($\phi = \pi/2$) can be seen from the focused mesh pattern at those locations. The symmetry plane passes through the middle of the surface crack in the y-z plane, but the crack face is curved to follow the fillet weld around the nozzle so both crack faces must be modeled in the crack mesh. The crack is located in the forefront of the mesh picture, at the low point of the fillet on the side of the shell.

For this example, the surface crack depth a is 0.25 in, and the surface crack length $2c$ is 1 in. The nozzle radius is 2 in, the nozzle length is 6 in, and the nozzle thickness is 0.5 in. The weld width and height are 0.6 in. The shell radius is 5 in, the shell thickness is 0.5 in, and the shell length is 10 in. The internal pressure is 200 psi. The tangential direction (around the cylinder) at the end of the nozzle and shell are constrained; this allows the nozzle and shell to expand due to internal pressure and sufficiently constrain the finite element mesh.

The *ANSYS* mesh currently requires a small radius keyhole to be used along the crack front to avoid element errors at the crack to fillet intersection. The small radius keyhole is typically used with non-linear geometry analyses, but can be used with caution for an elastic analysis. We recommend using *WARP3D* or *ABAQUS* to analyze geometries with the crack at the toe of the fillet weld.

Results are shown in Figures 6-3 through 6-6. The stress intensity K from displacement agrees overall with the K from the J-integral except at the crack tip ($\phi = 0$). Recall that at the crack tip a plane stress assumption is used to compute the K from displacement that may not be as accurate for the conditions at the toe of the fillet weld. The comparison of K from J and K from displacement is still very useful to verify that the J-integral results are valid. Comparing the K from J results from the three FEA programs shows close agreement in the result values.

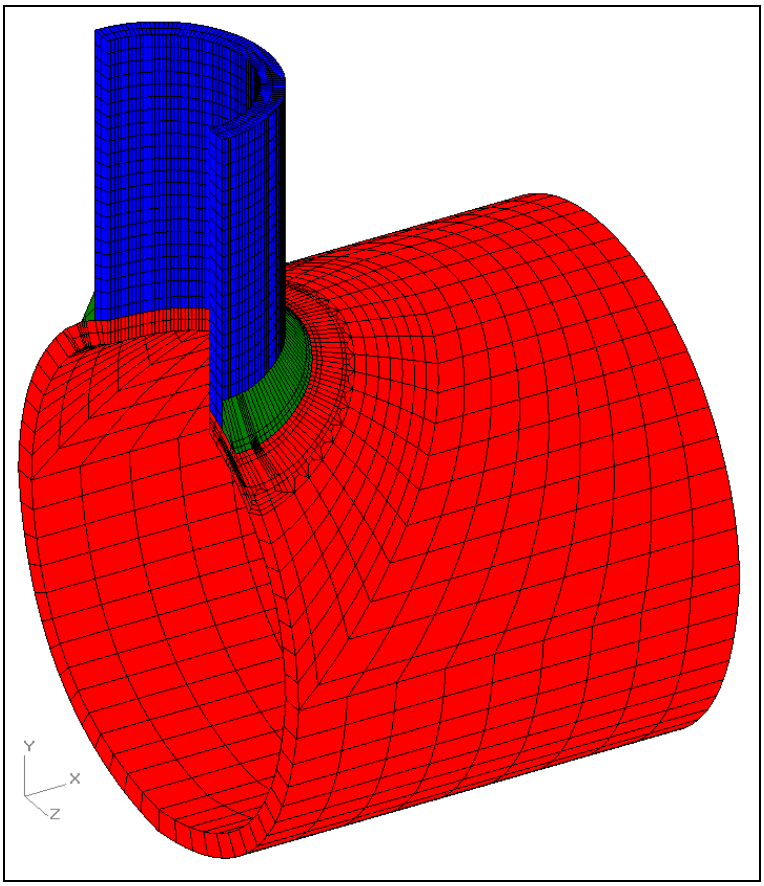

Figure 6-1. Nozzle with a surface crack at the toe of the fillet weld.

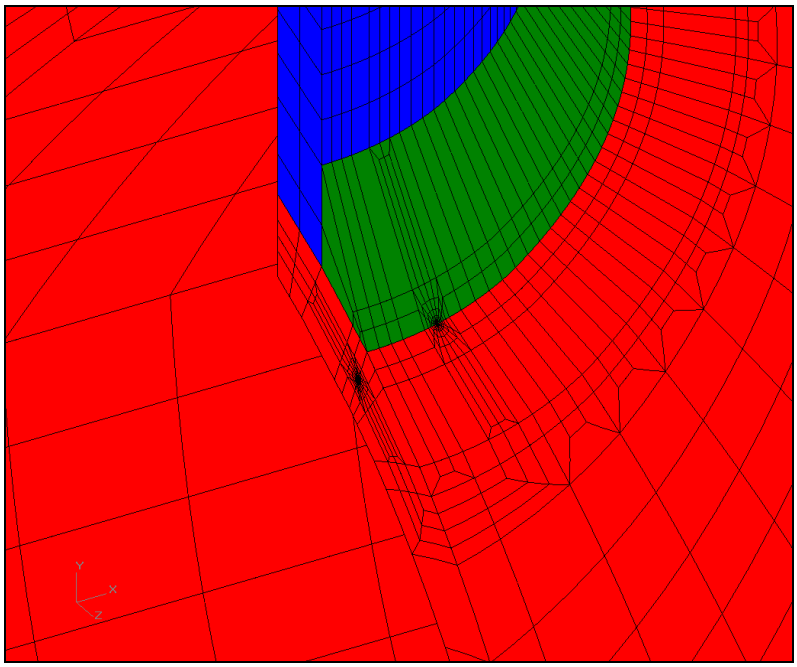

Figure 6-2. Close up of the surface crack in the shell at the toe of the fillet weld.

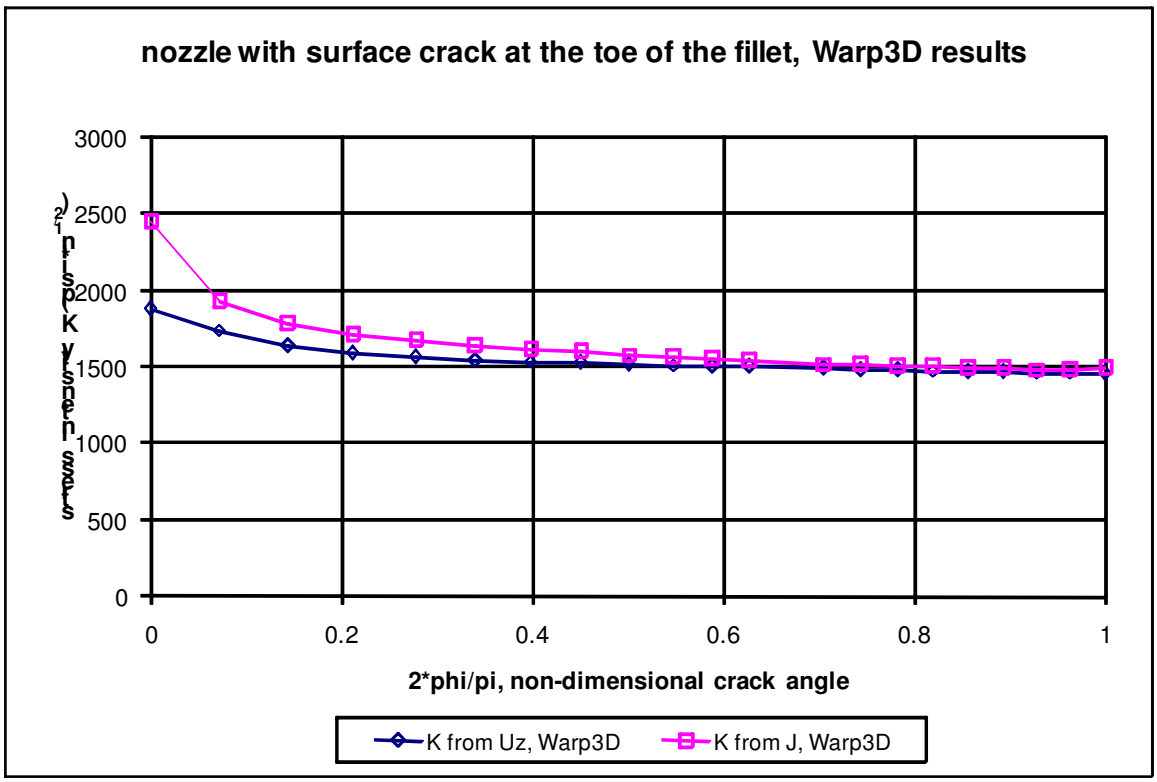

Figure 6-3. Compare *K* results for the nozzle, *WARP3D* results.

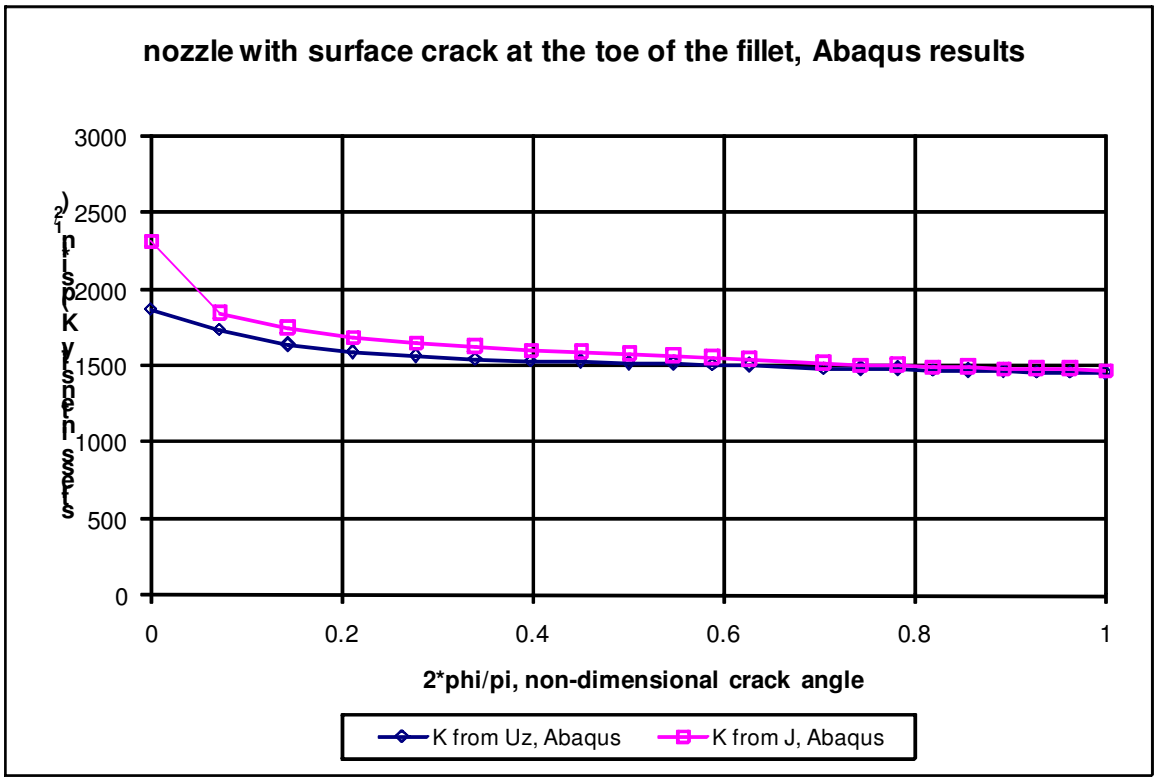

Figure 6-4. Compare *K* results for the nozzle, *ABAQUS* results.

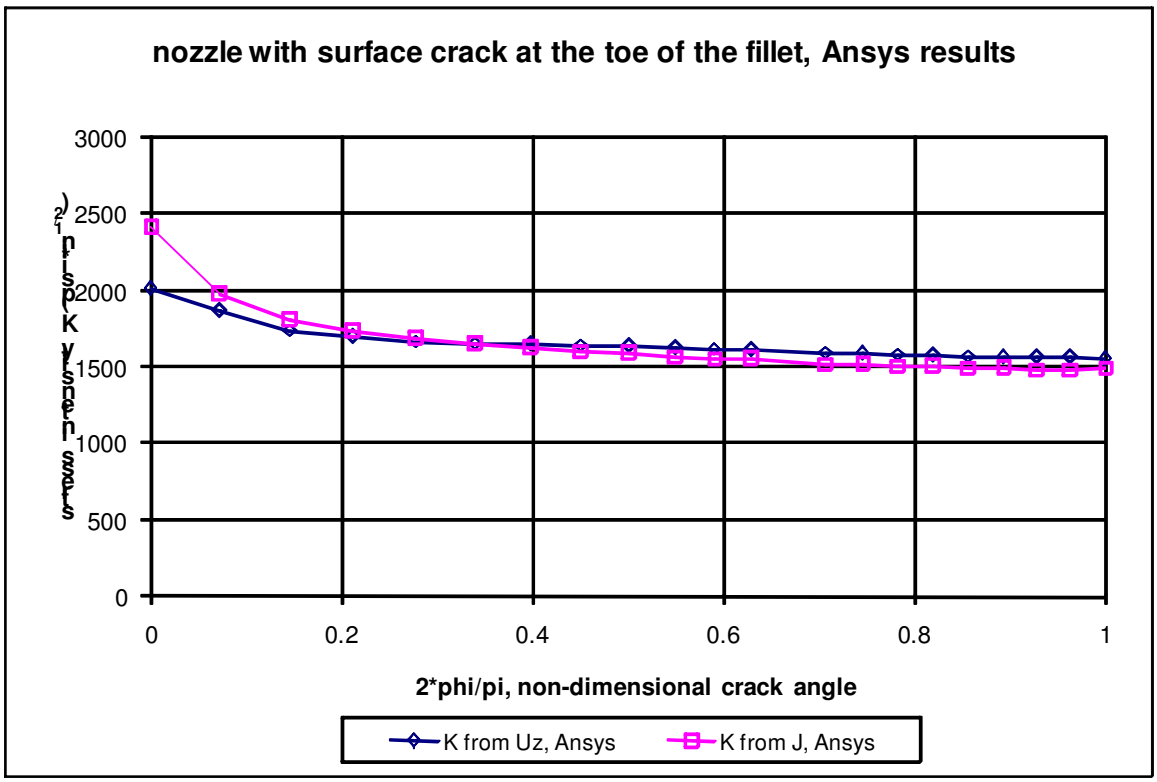

Figure 6-5. Compare *K* results for the nozzle, *ANSYS* results; small radius key hole used.

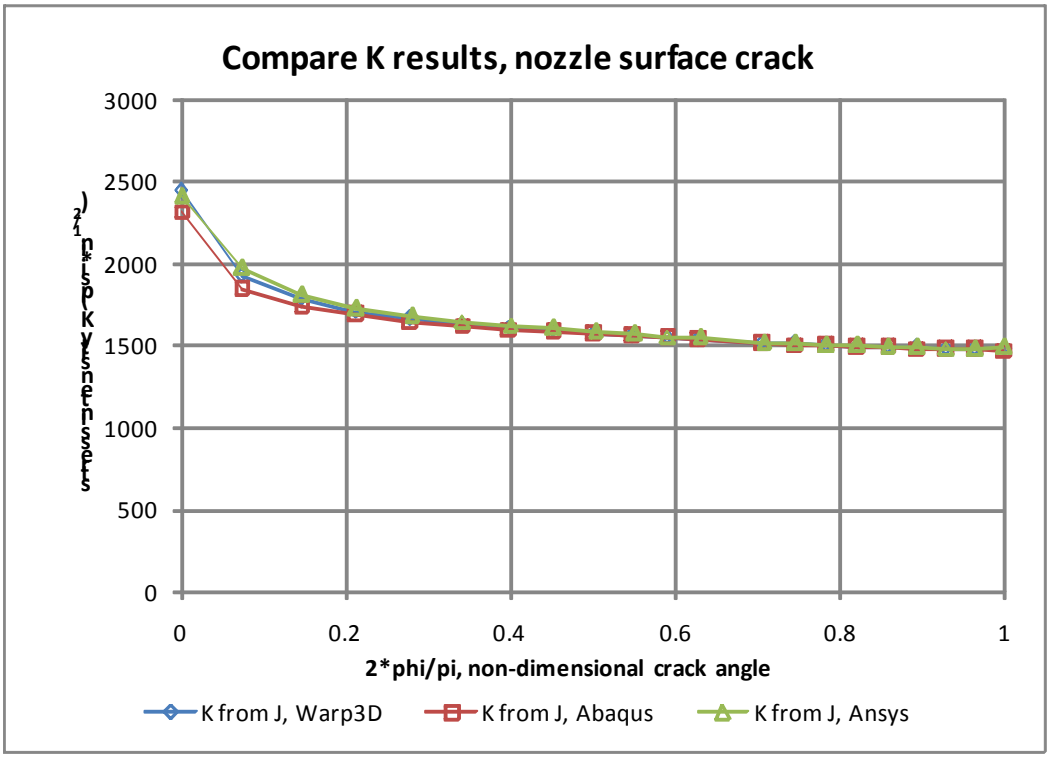

Figure 6-6. Compare crack results from each FEA program for the nozzle with a surface crack.

References

[1] Anderson, T. L., Fracture Mechanics, Fundamentals and Applications, 3rd ed., CRC Press, 2005, p. 49.

[2] Bergman, M. "Stress Intensity Factors for Circumferential Surface Cracks in Pipes." *Fatigue and Fracture of Engineering Materials and Structures*, Vol. 18, pp. 1155-1172, 1995.

[3] Anderson, p. 46.